

**Wettability Alteration by Chemical Agents at Elevated Temperatures and Pressures to
Improve Heavy-Oil Recovery**

by
You Wei

A thesis submitted in partial fulfillment of the requirements for the degree of
Master of Science
in
Petroleum Engineering

Department of Civil and Environmental Engineering
University of Alberta

© You Wei, 2017

Abstract

The thermal method is the primary method used to improve the recovery from reservoirs with heavy or extra-heavy oil. However, the efficiency and economic costliness of the traditional thermal process are limited by the unfavorable interfacial properties of heavy oil/water (steam)/rock system. Therefore, chemicals that can change the wettability and reduce the interfacial tension have been added to hot-water or steam to improve the efficiency of thermal recovery methods. This thesis aimed at screening thermal-resistant chemicals as interfacial modifiers to improve the heavy oil recovery and further investigating their working mechanism on the nanoscale.

Different types of new chemicals were tested in this study. High pH solution, ionic liquid, surfactants, and nanoparticles are evaluated by their thermal stability, interfacial alteration, and recovery improvement. The stability of the chemicals was tested through TGA (thermal gravimetric analysis) at steam temperature up 400°C. The theoretically optimized concentration that led to the lowest surface energy was achieved by measuring the interfacial tension between crude oil and solutions with a various concentrations. The suitability of the chemicals as wettability modifiers for different rock types was evaluated by contact angle measurements at high temperature and high pressure. Wettability alteration mechanism was further analyzed with atomic force microscopy (AFM), which provided the topography change of mica or calcite surface, which illustrated the deposition of the chemicals and removal of the existing oil layer. Imbibition tests were performed on sandstone and limestone cores with screened promising modifiers at 90 and 180°C.

Acknowledgements

As I draw near the end of my Master's study, the memories that were created along the way raised in my mind. First and foremost, I would like to express my appreciation to my supervisor Prof. Tayfun Babadagli for his continuous support and guidance on my Master's research, for his patience, encouragement, and trust.

I would also like to thank our technicians, Lixing Lin, Georgeta Istratescu and Todd Kinnee for their professional and patient help with my experiment. I am also thankful to Pamela Keegan for editing my thesis and papers, and to all the rest group members for their encouragement and inspiration.

I sincerely acknowledge the sponsorship from Prof. Tayfun Babadagli's NSERC Industrial Research Chair in Unconventional Oil Recovery (industrial partners are Petroleum Development Oman, Total E&P Recherche Développement, SIGNa Oilfield Canada, CNRL, SUNCOR, Touchstone Exploration, Sherritt Oil, PEMEX, Husky Energy, Saudi Aramco, Devon. and APEX Eng.) and an NSERC Discovery Grant (No: RES0011227).

I am thankful for all my friends at the University of Alberta, especially my two roommates Jessie and Ruixue. I couldn't be any luckier than to have you by my side during the past two years. I will never forget the times we shared the laughter and the sorrow.

Last but not the least, my special thank goes to my family: my parents and brother, for the support they provided me through my entire life. Without their support and encouragement, I would not have finished my Master's study.

Table of Content

Chapter 1: Introduction	1
1.1 Introduction.....	2
1.2 Statement of the Problem.....	3
1.3 Aims and Objectives.....	4
1.4 Structure of the Thesis	5
Chapter 2: Alteration of Interfacial Properties by Chemicals and Nano-Materials to Improve Heavy-Oil Recovery at Elevated Temperatures	6
2.1 Preface.....	7
2.2 Introduction.....	8
2.3 Materials and Methodology	10
2.3.1 Chemicals.....	10
2.3.2 Oil	10
2.3.3 Interfacial Tension	10
2.3.4 Contact Angle	11
2.3.5 AFM Test.....	12
2.3.6 Capillary Imbibition Tests	12
2.4 Results and Analysis.....	13
2.4.1 Interfacial Tension.	13
2.4.2 Contact Angle.	19
2.4.3 AFM Test.....	24
2.4.4 Capillary Imbibition.....	33
2.5 Conclusions.....	38
Chapter 3: Selection of New Generation Chemicals as Steam Additive for Cost Effective Heavy-Oil Recovery Applications	40
3.1 Preface.....	41
3.2 Introduction.....	42
3.3 Materials and Experiments	44
3.3.1 Oil phase	44

3.3.2 Aqueous phase	45
3.3.4 Substrates and cores	45
3.3.5 Thermogravimetric analysis (TGA).....	46
3.3.6 Contact angle and interfacial tension measurements	46
3.3.7 Capillary imbibition.....	47
3.4 Results.....	48
3.4.1 Thermogravimetric analysis.....	48
3.4.2 Contact angle measurements.....	49
3.4.3 Interfacial tension measurements.....	52
3.4.4 Capillary imbibition.....	54
3.5 Conclusions.....	61
Chapter 4: Conclusion and Future Work.....	62
4.1 Conclusions and Contributions.....	63
4.2 Limitations and Future Work.....	63
References	65

List of Figures

Figure 1. IFT device for interfacial tension and contact angle measurements.	11
Figure 2 Indiana limestone cores in Imbibition cells (before test).	12
Figure 3. Interfacial tension between crude oil and NaBO ₂ solution.....	14
Figure 4. Interfacial tension between crude oil and ionic liquid.....	15
Figure 5. Interfacial tension between crude oil and SiO ₂ nanofluid.....	16
Figure 6. Interfacial tension between crude oil and Al ₂ O ₃ nanofluid.	16
Figure 7. Interfacial tension between crude oil and C12TAB solution (left: measured at 25°C and interface age of 300 seconds; right: dynamic interfacial tension measured with a concentration of 0.75%wt).....	17
Figure 8. Temperature dependence of IFT in different solutions.	18
Figure 9. Contact angle results in tap water.....	19
Figure 10. Contact angle results on calcite.	20
Figure 11. Contact angle results on Indiana limestone.	21
Figure 12. Contact angle results on mica.....	22
Figure 13. Contact angle results on Berea sandstone.	22
Figure 14. Comprehensive effect of different chemical agents and temperature on capillary force..	23
Figure 15. 2D and 3D topography image of aged mica.....	24
Figure 16. 2D and 3D topography image of mica sample treated with tap water at 90°C for 20 hours.....	25
Figure 17. 2D and 3D topography image of mica sample treated with NaBO ₂ solution at 90°C for 20 hours.	26
Figure 18. 2D and 3D topography image of mica sample treated with ionic liquid solution at 90°C for 20 hours.....	26
Figure 19. 2D and 3D topography image of mica sample treated with C12TAB solution at 90°C for 20 hours.	27
Figure 20. 2D and 3D topography image of mica sample treated with SiO ₂ nanofluid at 90°C for 20 hours.	27

Figure 21. 2D and 3D topography image of mica sample treated with Al ₂ O ₃ nanofluid at 90°C for 20 hours.	28
Figure 22. 2D and 3D topography image of mica sample treated with ZrO ₂ nanofluid at 90°C for 20 hours.	28
Figure 23. 2D and 3D topography image of aged calcite.	29
Figure 24. 2D and 3D topography image of calcite sample treated with tap water at 90°C for 20 hours.	30
Figure 25. 2D and 3D topography image of calcite sample treated with NaBO ₂ solution at 90°C for 20 hours.	30
Figure 26. 2D and 3D topography image of calcite sample treated with ionic liquid solution at 90°C for 20 hours.	31
Figure 27. 2D and 3D topography image of calcite sample treated with C ₁₂ TAB solution at 90°C for 20 hours.	31
Figure 28. 2D and 3D topography image of calcite sample treated with SiO ₂ nanofluid at 90°C for 20 hours.	32
Figure 29. 2D and 3D topography image of calcite sample treated with Al ₂ O ₃ nanofluid at 90°C for 20 hours.	32
Figure 30. 2D and 3D topography image of calcite sample treated with ZrO ₂ nanofluid at 90°C for 20 hours.	33
Figure 31. Oil recovery vs. time in limestone cores at 90°C.	33
Figure 32. Surface properties and capillary force for limestone at 90°C.	34
Figure 33. Nanofluid is unstable at 90°C (left: SiO ₂ , middle: Al ₂ O ₃ ; right: ZrO ₂).	35
Figure 34. Comparison of production in 10 days at 25°C (Mohammed and Babadagli 2014) and 90°C.	36
Figure 35. Oil recovery vs. time in sandstone cores at 35°C.	37
Figure 36. Surface properties and capillary force for sandstone at 90°C: (a) Contact angle and interfacial tension; (b) capillary force.	38
Figure 37. IFT setup used to measure IFT and contact angle.	47
Figure 38. High-temperature high-pressure imbibition setup.	48
Figure 39. Thermogravimetric analysis of tested chemicals.	49

Figure 40. Contact angle on calcite and Indiana limestone measured at 180°C.....	50
Figure 41. Contact angle on calcite and Indiana limestone measured at 180°C.....	51
Figure 42. Comparison of contact angles at 25°C, 90°C (from Wei and Babadagli 2016), and 180°C.	52
Figure 43. Oil droplets on calcite surface in C12TAB solution at 60°C, 90°C, and 120°C.	52
Figure 44. IFT between oil and different chemical solution at 180°C and 185 psi.	53
Figure 45. Comparison of IFT at 25°C, 60°C and 90°C, 14.7 psi (from Wei and Babadagli, 2016)..	54
Figure 46. Oil recovery vs. time from limestone cores in tap water at 180°C.	55
Figure 47. Oil recovery vs. time in limestone cores at 180°C and 185 psi.....	56
Figure 48. Summary of surface properties in oil/ limestone solutions at 180°C and 185 psi.....	57
Figure 49. Oil recovery vs. time in sandstone cores at 180°C and 185 psi.	59
Figure 50. Summary of surface properties in oil/ sandstone solutions at 180°C and 185 psi.	60

List of Tables

Table 1. List of Chemicals Used in Chapter 2	10
Table 2. Temperature and Pressure Values for Contact Angle Measurement	11
Table 3. Limestone Imbibition Experiment Data	13
Table 4. Sandstone Imbibition Experiment Data	13
Table 5. Optimum Chemical Concentration based on Interfacial Tension Results	18
Table 6. Surface Roughness Parameters of Different Mica Surface	24
Table 7. Surface Roughness Parameters of Different Calcite Surface	29
Table 8. List of Tested Chemicals in Chapter 3.....	45
Table 9. Limestone Imbibition Experiment Data.	46
Table 10. Sandstone imbibition Experiment Data.	46
Table 11. Weight Fraction at 180°C.	49
Table 12. Contact Angles of Oil in Tap Water at 25°C, 90°C (from Wei and Babadagli 2016) and 180°C.	49

Chapter 1: Introduction

1.1 Introduction

As conventional oil reserves continuously decline, the exploitation of heavy oil reservoir has become increasingly popular. The primary technique to enhance heavy oil recovery is viscosity reduction of heavy oil by injecting hot water or steam into the reservoir. However, for more challenging heavy or extra-heavy oil reservoirs with unfavourable interfacial properties, strong oil-wetness of the rock and high surface energy between oil and displacing phase are the other two critical factors that impair the efficiency increase cost of thermal recovery. Therefore, using proper additives in the hot-water or steam to improve the performance of traditional thermal process has been widely studied in the literature. Early attempts include the combination of thermal recovery and surfactant flooding (Green and Malcolm 1985; Handy et al. 1982; Maini and Ma 1985) or solvent injection (Frauenfeld et al. 2007; Sharma and Gates 2013). In recent years, more efforts have been placed on new generation chemicals that can efficiently improve the wettability and reduce the interfacial tension of the oil/hot-water (rock)/rock system.

Wettability of the rock is a critical factor that affects the flowing pattern in the reservoir. The potential to increase recovery by wettability alteration is significant, as 84% of carbonate reservoirs in the world are thought to be oil-wet (Wang et al. 2011). The two main methods to change wettability in the reservoir are chemical and thermal. Chemical method is the topic of this study, while the thermal is significant when the target is heavy oil reservoir.

Interfacial tension between oil and water (steam) is another important parameter in immiscible displacement. A significant increase in the final recovery factor is obtained in core flooding experiments when the interfacial tension is sufficiently reduced (Wagner and Leach 1966). Interfacial tension is influenced by many factors, including temperature, pressure, composition of the crude oil, and additives in injected fluid. Surfactants are widely used in tertiary recovery because of their efficiency in reducing interfacial tension as ultralow IFT (lower than 10^{-3} mN/m) is reported to be possible at a low surfactant concentration (Wade et al. 1977; Hayes et al. 1979).

1.2 Statement of the Problem

Thermal recovery methods have been widely applied to heavy oil reservoirs. The mobility of heavy can be improved by injecting hot-water or steam into the reservoirs. However, for oil-wet rock reservoirs, the rate and extent of recovery are limited. Therefore, changing the wettability of the heavy-oil reservoir is critical and necessary to improve the efficiency of the thermal process. The significance of wettability on recovery was pointed out as early as 1942 (Buckley and Leverett). Since then, wettability alteration using chemical agents in conventional reservoirs has been widely studied. Different types of chemicals have been tested in laboratory and field. Mohammed and Babadagli (2015) systematically summarized potential wettability alteration chemical agents and approaches. However, the alteration of wettability in the heavy-oil system is undoubtedly more challenge and complicated for the following reasons:

1. The use of traditional wettability modifiers, like surfactants, are limited because many of them are unstable at high temperature. Novel thermal resistant chemicals are needed to change the wettability of reservoirs during the thermal recovery process.
2. Aside from wettability, the interfacial tension between heavy oil and displacing phase is also affected by temperature and the addition of chemicals. With interfacial tension, wettability interact with each other and are both affected by temperature, making it hard to identify the contributions of chemicals and temperature.

For the first challenge, some new promising chemicals were suggested as modifiers at high temperature. Chen and Mohanty (2014), for example, found anionic surfactant exhibited high capability in wettability alteration in the existence of chelating agents at temperatures lower than 120°C; however, the formulation was not tested at higher (steam) temperatures. Cao et al. (2016) evaluate the capabilities of high pH solution, imidazolium ionic liquid, a cationic surfactant, and nanoparticles on changing the wettability of different rock plates and mineral substrates at temperatures up to 200°C. The wettability alteration was identified quantitatively by contact angle measurements but the analysis of the change of interfacial tension was ignored and the study of the working mechanism was missing.

For the second challenge, capillary imbibition tests were adopted as an efficient method to investigate the comprehensive effect of chemical agents and temperature in the laboratory.

However, the application of imbibition is limited to a temperature lower than 100°C due to the restriction of Amott cell.

The limitation of previous research turned our attention to these four important issues:

1. Which chemicals are capable of altering the wettability of sandstone and carbonates at elevated temperature?
2. Which mechanisms of wettability alteration are induced by different types of chemical agents?
3. How is the interfacial tension between oil and displacing fluid influenced by chemicals, pressure, and temperature?
4. How are the rate and extent of recovery affected by different chemicals at high temperature and high pressure?

1.3 Aims and Objectives

This research aims to perform the following objectives:

1. To design an experimental setup for the capillary imbibition at high temperature and high pressure;
2. To study the effect of temperature and concentration on the interfacial tension between oil and solutions of following chemicals:
 - High pH solution
 - Ionic liquid
 - Cationic surfactant
 - Nano-fluids;
3. To study the influence on interfacial tension and get the optimized concentration of solutions to get lowest interfacial tension of the following factors:
 - Chemical additives
 - Concentration
 - Temperature
 - Pressure;
4. To quantitatively evaluate the wettability alteration induced by chemicals at temperatures up to 200°C on different types of rocks;

5. To illustrate the mechanism of wettability alteration of different chemical solutions on nano scale;
6. To screen suitable chemicals to enhance the recovery from sandstone and carbonate at hot-water temperature and steam temperature.

1.4 Structure of the Thesis

This is a paper-based thesis consisting of four chapters. Chapter 2 and Chapter 3 are two papers that were presented at conferences and submitted for peer review.

Chapter 1

This chapter is an introduction to this thesis. The significance of wettability alteration in heavy oil reservoir is demonstrated first. Then the limitation of previous research is discussed, followed by the objectives of this thesis.

Chapter 2

The concentrations of selected chemical solutions were optimized based on the interfacial tension results. The capability of selected chemicals as wettability modifiers were evaluated by contact angle measurement. The mechanisms of wettability alteration were further explained by the adsorption or removal of chemicals and oil on rocks on nanoscale. Then, capillary imbibition tests were conducted in sandstone and limestone to analyze the roles of capillary and gravity forces in oil recovery process at a hot-water temperature (90°C).

Chapter 3

A new experiment setup was designed for imbibition test to study the comprehensive effect of chemicals, temperature, and pressure on production at a steam temperature (180°C). The thermal stability of chemical agents was tested with TGA. The effect of chemicals on wettability and interfacial tension at high temperature and high pressure were evaluated separately.

Chapter 4

This chapter summarizes the contributions of this thesis. The limitations are also listed for the improvement in future work.

Chapter 2: Alteration of Interfacial Properties by Chemicals and Nano-Materials to Improve Heavy-Oil Recovery at Elevated Temperatures

This paper is a modified version of SPE 181209, which was presented at SPE Latin America and Caribbean Heavy and Extra Heavy Oil Conference held in Lima, Peru, 19-20 October 2016. A version of this paper has been submitted to Energy and Fuels for publication.

2.1 Preface

Heavy oil containing carbonate and sand reservoirs exhibits reverse wettability characteristics. Depending on temperature, the phase of injected steam, and rock type, the wettability may be altered to more water-wet. The addition of chemicals to hot-water (or steam) may further change the interfacial properties (more water-wet and less interfacial tension). Surfactants were tested extensively for this process in the past and their temperature resistance was an obstacle. New generation chemicals need further investigation from a technically and economically success point of view.

The objective was to investigate the alteration of interfacial properties induced by different types of chemical agents under high temperature conditions. To achieve this, four experimental tools (contact angle measurement, interfacial tension measurement, atomic force microscopy and spontaneous imbibition tests) were applied. High pressure and high temperature contact angle measurements enabled a quick method to identify the suitability of the chemicals for wettability modification. Interfacial tension between oil and the different chemical solution was measured with a variation of temperatures. In the imbibition tests, core samples were exposed to heating for longer time periods so that the temperature resistance of the chemicals was also tested. Imbibition experiments were conducted at ambient pressure and 90°C. The combination of the contact angle and interfacial tension provided insight into the recovery enhancement mechanisms.

Six different chemicals including an ionic liquid, three nano-fluids (silica, aluminum, and zirconium oxides), a cationic surfactant, and a high pH solution were chosen based on our screening study. Heavy-oil used was obtained from a field in Alberta, Canada (6,000cp). Contact angles were measured on mica, calcite, sandstones and limestones plates. The experimental temperature ranged from 25 to 200°C and pressure was changed to keep the solution in the aqueous phase. Promising modifiers for different rock types under different temperatures were screened separately. Visual data illustrating the deposition of the chemicals on the surface of mica and well-polished calcite substrates, and removal of the existing oil layer after the treatment with different chemicals were obtained by atomic force microscopy (AFM). Finally, spontaneous imbibition tests were performed on sandstone and limestone cores with screened promising modifiers. Oil recovery in this phase was continuously monitored to evaluate wettability

alteration capability and the mechanism(s) involved was analyzed for different chemicals. Analysis of wettability alteration mechanisms and IFT reduction capabilities is expected to be useful in the selection of suitable and temperature-resistant chemicals for high temperature applications in different reservoir rocks.

2.2 Introduction

It is well known that the extent and rate of oil recovery are controlled by the interplay of three forces: capillary, viscous, and gravity. Reducing viscous force is always the main task when exploring heavy oil reservoir. Hence, thermal recovery methods are designed to lessen the viscosity of heavy oil by increasing temperature. Solvent based methods are another option to reduce viscosity and have been well studied (Edmunds et al. 2009; Jiang et al. 2010). A combination of these methods was also applied successfully at the laboratory scale (Naderi et al. 2013). However, for more challenging heavy oil reservoir with the oil-wet or mixed-wet state, reducing viscosity alone is not sufficient to recover oil efficiently and economically. Different chemical agents have been tested and used to alter wettability of reservoir rock and improve interfacial tension during the thermal recovery process to enhance capillary and gravity driven recovery mechanisms.

When chemical is applied at different temperatures, wettability and interfacial tension interact with each other and are both affected by temperature (Hamouda and Gomari 2006; Chen and Mohanty 2014, Schembre et al. 2016). This means they are not independent of each other and their partial contribution to the process should be identified. The interplay of these three factors makes the analysis of chemical assisted thermal recovery processes complicated. In this work, selected chemical agents in previous studies (Mohammed and Babadagli 2015a; Cao et al. 2015) including high pH solution, ionic liquid, cationic surfactant, and nano-fluids were studied to identify their influence on surface wettability and interfacial tension change at different temperatures.

During high pH solution or alkaline injection for enhanced oil recovery, different mechanisms including in situ surfactant formation and wettability alteration may play a role (Mohammed and Babadagli 2015b). Wettability alteration during this process occurs by decreased positive charge of carbonates making the surface less attractive to the negatively charged part of crude oil

(Mohammed and Babadagli 2015a). $NaBO_2$ (sodium metaborate) was selected to prepare the high pH solution in this study as it was observed to have a better capability of improving oil recovery than other alkalis solutions (like NaOH) with the same initial pH of 11.5 (Mohammed and Babadagli 2015ab; Zhang and Nguyen 2008).

Ionic liquids, which refer to salts that have low melting temperature and relatively low viscosity, are widely studied in the area of oil sand extraction (Wasserscheid and Keim 2000). This type of chemical is believed to be capable of reducing IFT and adhesive forces changing surface properties of oil/ionic and liquid/rock systems. Hogshead et al. (2011) verified this by measuring interaction forces between bitumen and a silica probe. The force was about an order smaller in ionic liquid $[BMMIM][BF_4]$ than other surface active agents. This reduction was contributed to ion/charge layers formed on the top of surface.

Nano fluids are defined as fluids with dispersed nano-sized materials; i.e., they form nanoscale colloidal suspensions with condensed nanoparticles (Yu and Xie 2012). Nanoparticles have been popular in recent years because of their capability of enhancing thermophysical properties at low cost (Ayatollahi and Zerafat 2012). The capability of nanoparticles to alter contact angle and interfacial tension has been proved by a lot of lab work (Torsater et al. 2012; Ragab and Hannora 2015; Li et al. 2015, Roustaei and Bagherzadeh 2015). Maghzi et al. (2011) observed that the residual oil in pores and throats were significantly reduced after silica nanoparticles were added into the polymer solution. They suggested that wettability was changed to more water-wet because of the adsorption of silica nanoparticles on the surface. The adsorption behavior of nanoparticles has been the focus of several studies. Wasan and Nikolov (2003) observed a film of nanoparticle at three phases contact region. Karimi et al. (2012) suggested that hydrophilic nanoparticles with high surface energy can form nano-textured ribbons on solid.

The objective of this work is to select a proper chemical to improve the performance of thermal applications in sands and carbonates. The effect of new chemical agents on interface properties was evaluated by interfacial tension and contact angle measurements for heavy-oil/chemical solution/rock systems. The interfacial tension in different chemical solutions was measured with a variation of temperature and concentration. For the contact angle tests, special attention was given to the effect of temperature. Contact angle measurements were conducted at a temperature

range varying from 25 to 200°C, which is close to a typical steam injection temperature. In addition to these, capillary imbibition tests were carried out to demonstrate the roles of capillary and gravity forces in oil recovery process under static conditions. Imbibition behaviour in different solutions was combined with the results of surface property alteration to identify the mechanism of recovery enhancement by different chemical agents.

2.3 Materials and Methodology

2.3.1 Chemicals. Including tap water as a base case, seven chemical solutions were tested in this study, listed in **Table 1**. The cationic surfactants tested were C₁₂TAB (chemical formula: n – C₂₃H₂₅N(CH₃)₃Br). Three nanofluids, silicon oxide, aluminum oxide, and zirconium oxide were used in imbibition tests. But, interfacial tension and contact angle measurements were performed for only the first two due to the very cloudy nature of zirconium oxide, which prohibited obtaining any quality images. Silicon oxide, aluminum oxide, and zirconium oxide nanofluids were prepared with nanopowder with sizes of 5-35 nm, 10 nm, and 45-55 nm, respectively. All solutions were prepared by weighting chemical agents in distilled water and stirring with a magnetic stirrer at ambient temperature.

Table 1. List of Chemicals

Chemical type	Chemical name
Base case	Tap Water
High pH solution	Sodium metaborate (<i>NaBO₂</i>)
Ionic liquid	1-Butyl-2,3-dimethylimidazolium tetrafluoroborate (<i>BMMIM BF₄</i>)
Cationic surfactant	C12TAB
Nanofluids	Silicon Oxide (<i>SiO₂</i>)
	Aluminum Oxide (<i>Al₂O₃</i>)
	Zirconium Oxide (<i>ZrO₂</i>)

2.3.2 Oil. Heavy crude oil from a field in eastern Alberta, Canada was used as the oil phase in all experiments. The oil had a viscosity of 6,000 cp and API gravity of 13° at 25°C.

2.3.3 Interfacial Tension. Interfacial tension was measured at a temperature range of 25 to 90°C using a pendant drop device (**Figure 1**). Pressure cell was first filled with the chemical solution. Then an oil droplet was injected from the bottom with a stainless steel needle. Pictures of drop shapes were taken by the camera and analyzed by software (DROPimage Advanced program). For each chemical agent, measurements were carried out at different concentrations. The

concentration that led to the lowest interfacial tension values were used in contact angle measurement and capillary imbibition tests.

2.3.4 Contact Angle. Four representative surfaces of sandstones (mica plate and Berea sandstone) and carbonates (calcite plate and Indiana limestone) were used in the contact angle measurements. Calcite plates were cut from a calcite block along the cleavage plane. Berea sandstone Indiana limestone substrates were first cut from core plugs and polished to obtain relatively smooth surfaces. All mineral plates and rock substrates were aged in the crude oil for two weeks at 70°C. After removing extra oil carefully with toluene, they were dried at ambient temperature for two days.

The contact angle was measured at static conditions to assess the wettability of surfaces when different chemical solutions are used. Measurements were done in the IFT device (**Figure 1**) at temperatures ranging from 25 to 200°C. Pressure was increased accordingly to maintain water in a liquid phase (**Table 2**).

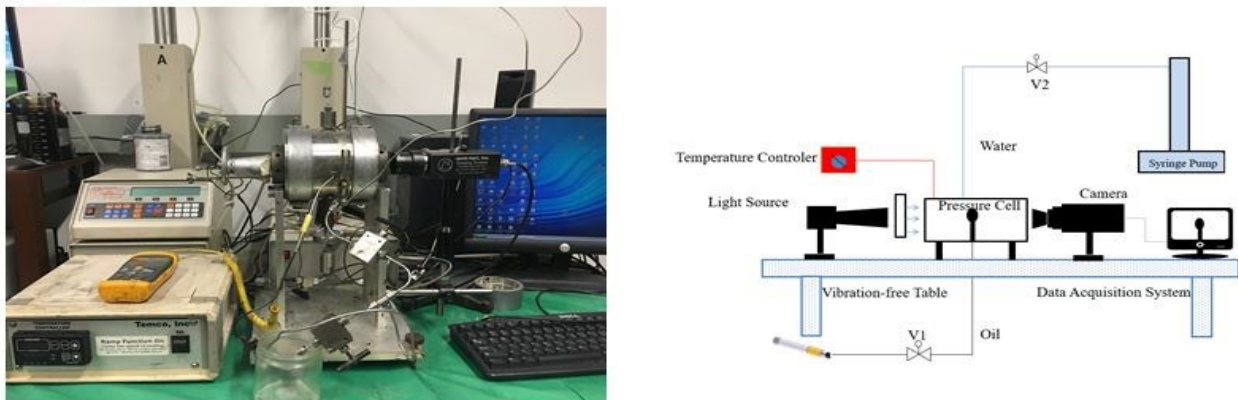


Figure 1. IFT device for interfacial tension and contact angle measurements.

Table 2. Temperature and Pressure Values for Contact Angle Measurement

Temperature, °C	Pressure, psi
25	14.7
60	30
90	50
120	200
160	250
200	300

2.3.5 AFM Test. Mica and calcite plates were used in the AFM tests. Mica surface was atomically smooth, while calcite surface was polished before the treatment. All mineral plates were aged in crude oil at 70°C for five days. Then, the samples were centrifuged at the speed of 8000 rpm for 1 hour at 40°C to remove extra oil. To study the effects of different solutions on surface properties, samples were then soaked in different solutions at 90°C for 20 hours. Next, the plates were washed with distilled water and dried at ambient temperature. Each plate was scanned in the air before and after the treatment with a chemical solution. The microscope used in this research was the Dimension® Icon™ Scanning Probe Microscope (SPM). Both mica samples and calcite samples were scanned with contact probes. Original data used was analysis with software NanoScope Analysis 1.40.

2.3.6 Capillary Imbibition Tests. Berea sandstone and Indiana limestone cores were saturated in crude oil for one week at 80°C. Then, cores were aged in oil at 80°C. Limestone cores were aged for two weeks to establish an oil-wet state, while sandstone cores were aged for five weeks due to their more water-wet nature compared to the limestone samples. Saturated cores were placed into imbibition cells containing tap water and different chemical solution (**Figure 2**). The cells were put in the oven at a temperature of 90°C and ambient pressure. Oil expelled from cores was recorded versus time. Detailed data for imbibition tests on Indiana limestone cores and Berea sandstone cores are listed **Table 3** and **Table 4** respectively.



Figure 2. Indiana limestone cores in Imbibition cells (before the test).

Table 3. Limestone Imbibition Experiment Data

	Core diam., mm	Core height, mm	PV, cm^3	Porosity, %	Chemical	Conc., %wt
L1	38.5	87.5	10.65	10.46	Tap water	
L2	38.5	87.1	10.82	10.68	$NaBO_2$	1.50
L3	38.0	87.2	11.32	11.45	Ionic liquid	1.00
L4	38.0	87.1	10.62	10.76	C12TAB	0.75
L5	37.9	87.2	10.60	10.78	SiO_2	1.00
L6	37.8	87.2	10.31	10.54	Al_2O_3	0.75
L7	38.1	87.3	10.94	11.00	ZrO_2	1.00

Table 4. Sandstone Imbibition Experiment Data

	Core diam., mm	Core height, mm	PV, cm^3	Porosity, %	Chemical	Conc., %wt
S1	37.9	87.5	16.90	17.23	Tap water	
S2	38.0	86.5	17.12	17.38	$NaBO_2$	1.50
S3	38.0	87.5	15.66	15.88	Ionic liquid	1.00
S4	37.9	86.0	15.42	16.18	C12TAB	0.75
S5	37.9	85.0	19.07	19.62	SiO_2	1.00
S6	37.6	87.5	15.26	15.79	Al_2O_3	0.75
S7	37.6	87.0	14.99	15.29	ZrO_2	1.00

2.4 Results and Analysis

The results of interfacial tension and contact angle measurements are presented in graphical form below. Note that a limited number of experiments were repeated using different droplet and the results are indicated using error bars. Due to the intensity and highly time-consuming nature of the experiments, only multiple measurements were made (10-15 times) using the same droplet and an average value is used in the plots. These points do not have error bars. The same approach was applied in the contact angle measurements.

2.4.1 Interfacial Tension. The interfacial tension between crude oil and solution is affected by many factors, including temperature, pressure, and the composition of oil. In this study, interfacial tension between oil and solution was measured with a variation of temperature and concentration. The concentration value that yielded the lowest interfacial tension was used in further contact angle and imbibition tests.

Interfacial tension between crude oil and $NaBO_2$ solution was measured at a temperature range of 25 to 90°C. The concentration was changed from 0.5% wt to 2.0% wt. **Figure 3a** shows the

effect of temperature on interfacial tension between crude oil and $NaBO_2$ solution with different concentrations. Interfacial tension decreases by increasing temperature systematically for all cases. At different temperatures, the lowest interfacial tension value was observed at the concentration range of 1% to 1.5%wt (**Figure 3b**).

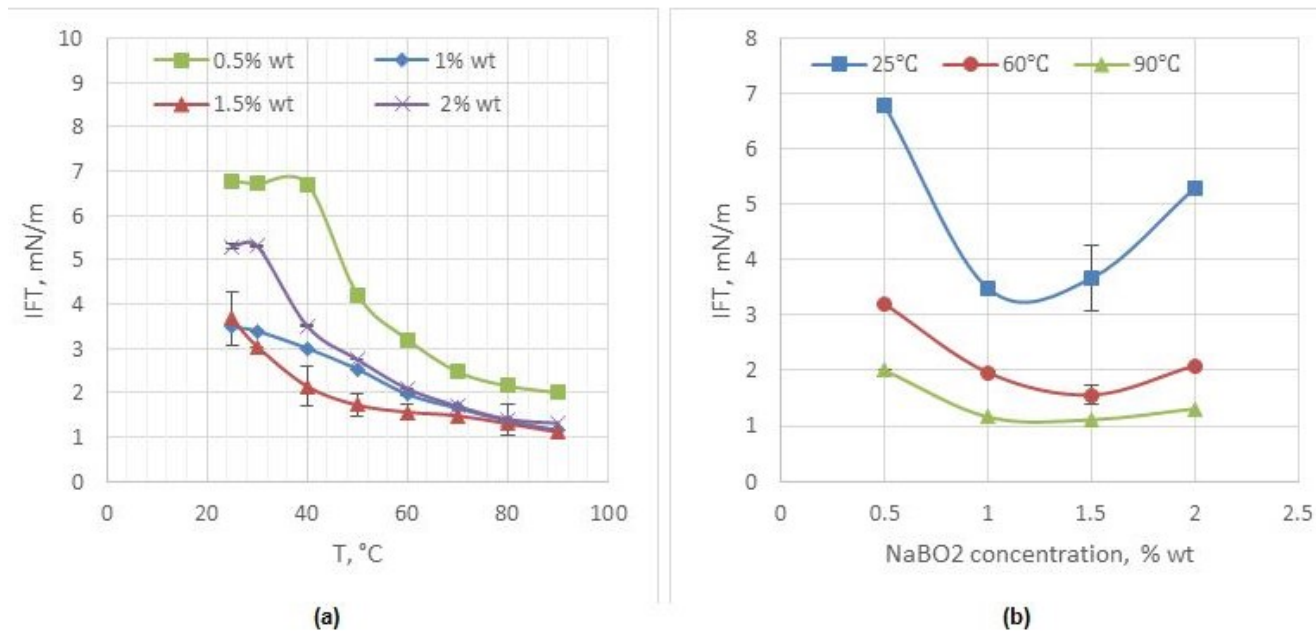


Figure 3. Interfacial tension between crude oil and $NaBO_2$ solution.

Measurement results show that $[BMMIM][BF_4]$ solution with concentration of 0.5%wt yields a reduction of interfacial tension from 28.35 to 6.94 mN/m at 25°C and higher concentrations are not needed. Interfacial tension between oil and solution linearly decreases with temperature increasing (**Figure 4a**) for a given temperature range. Higher temperature benefits the adsorption of $[BMMIM][BF_4]$ molecules onto the interface, thus causing lower interfacial tension. As shown in **Figure 4b**, interfacial tension values almost remains constant in the concentration range of 0.5% wt to 1.5% wt. Here concentration 1.0% wt was chosen for the contact angle and imbibition tests also considering the earlier test results reported elsewhere (Mohammed and Babadagli 2015a; Cao et al. 2015).

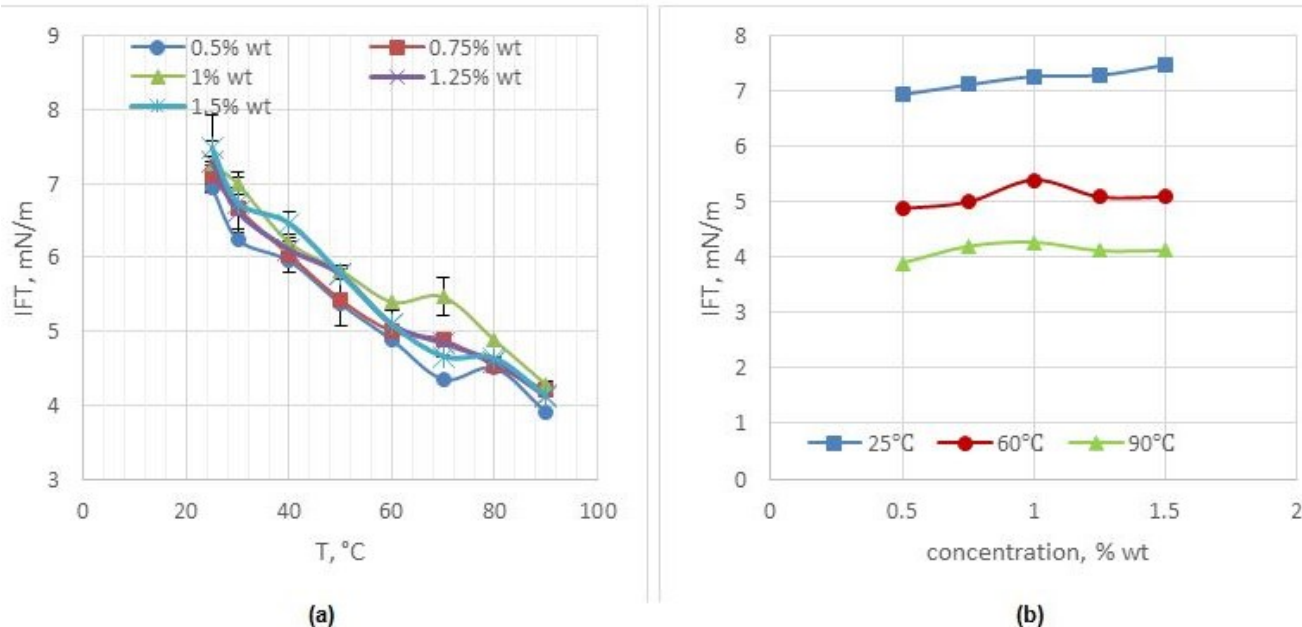


Figure 4. Interfacial tension between crude oil and ionic liquid.

It is well accepted that suitable nanoparticles can adsorb at the liquid-liquid interface. However, their effect on interfacial tension has long been in dispute. According to the results of this work (**Figure 5a** and **Figure 6a**), both SiO_2 and Al_2O_3 nanoparticles can significantly reduce the interfacial tension at low temperatures. Moreover, with the same concentration, SiO_2 nanoparticle was more efficient in reducing interfacial tension than Al_2O_3 nanoparticle.

Figure 5a shows the temperature dependence of interfacial tension in SiO_2 nanofluid. One interesting observation is that the interfacial tension between oil and SiO_2 nanofluid undergoes a minimum value with the increase of temperature. This temperature corresponding to lowest interfacial tension is known as phase inversion temperature. When temperature is below phase inversion temperature, adsorption of nanoparticles is increased by increasing temperature. Minimum interfacial tension is reached at phase inversion temperature when adsorption of nanoparticles on the surface reaches the maximum. For temperature higher than phase inversion temperature, adsorption is impaired, thus interfacial tension increases. No significant change was observed when concentration was changed (Figure 5b).

In Al_2O_3 nanofluid, the interfacial tension increases with increasing temperature (Figure 6a) because of thermal instability. Hence, the actual concentration of Al_2O_3 nanofluids that contacted oil droplet during measurement was lower than the original concentration.

SiO_2 nanofluid gave the lowest interfacial tension with concentration of 1%wt, while Al_2O_3 nanofluid had the strongest IFT-reducing capability at 0.75%wt (Figure 5b and Figure 6b).

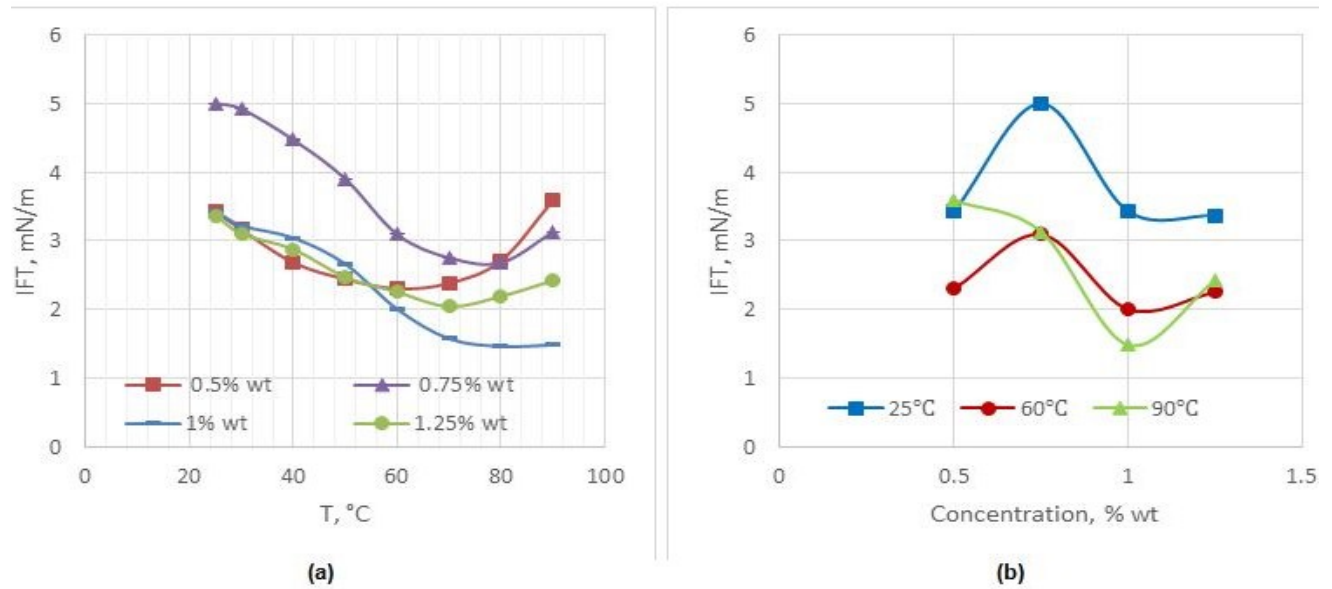


Figure 5. Interfacial tension between crude oil and SiO_2 nanofluid.

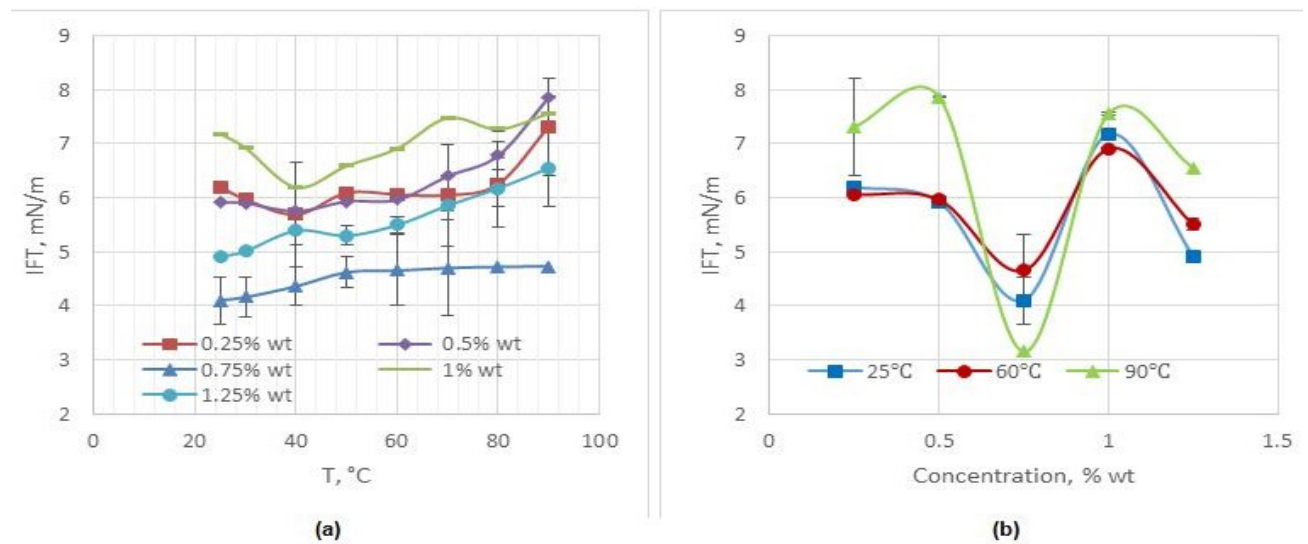


Figure 6. Interfacial tension between crude oil and Al_2O_3 nanofluid.

The cationic surfactant can efficiently reduce interfacial tension by its adsorption on the interface. The actual values of interfacial tension should be lower than the values plotted in **Figure 7a**, which were measured before equilibrium (at a surface age of 300 seconds). This is because actual interfacial tension values are lower than our minimum measurable value, which is determined by the diameter of the tip in the pendent-drop method. However, we can observe through Figure 7a the dependence of interfacial tension on C12TAB concentration. The tension between oil and C12TAB solution surface decreases with the increase of concentration. The CMC value of C12TAB is reported as 0.43%wt in distilled water at 25°C in the literature (Wasserscheid and Keim et al. 2000). In this case, minimum value was not reached around 0.43% wt. A similar phenomenon was observed by Ye et al. (2012) and was attributed to the existence of material polarity in the oil phase. Lower interfacial tension is expectable with a concentration higher than 1% wt. However, based on economic consideration, 0.75%wt was chosen for further experiments. **Figure 7b** shows the dynamic interfacial tension between oil and 0.75%wt C12TAB at different temperatures. Based on the trend of three curves, it is reasonable to speculate that interfacial tension in C12TAB increases with an increase in temperature.

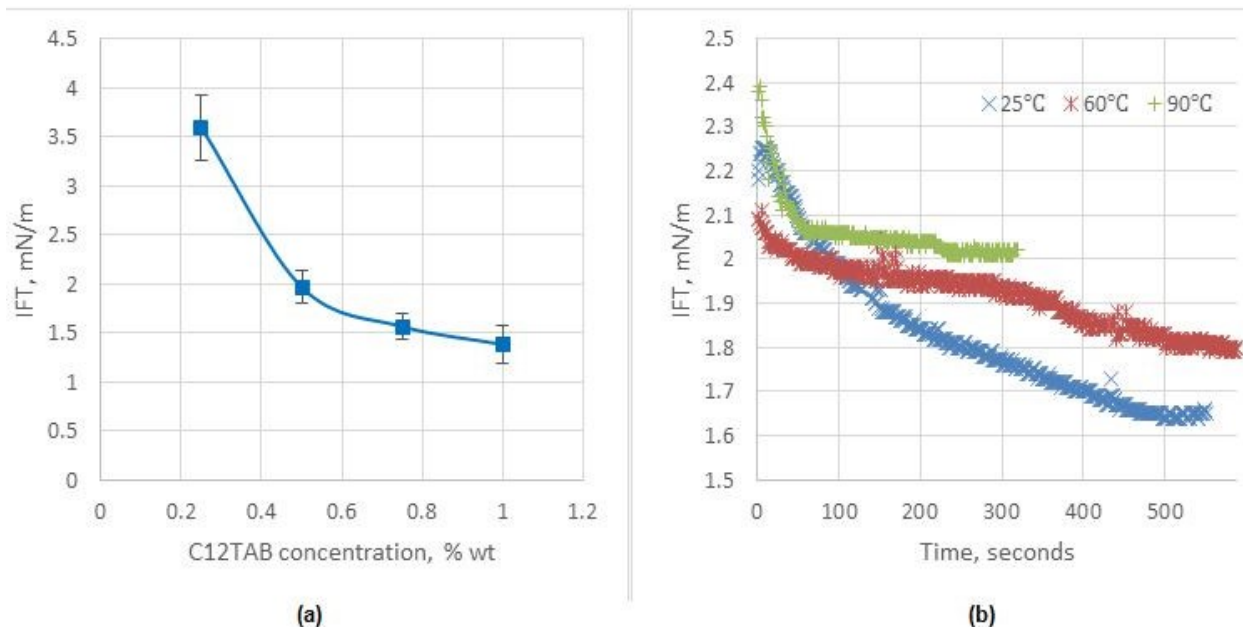


Figure 7. Interfacial tension between crude oil and C12TAB solution (left: measured at 25°C and interface age of 300 seconds; right: dynamic interfacial tension measured with a concentration of 0.75%wt).

The selected concentrations of each kind of chemical solution are summarized in **Table 5**. Those concentrations were used in the following contact angle tests, AFM tests, and capillary imbibition tests. **Figure 8** summarizes the effect of temperature on the interfacial tension in different solutions. One may observe that all chemical agents led to a lower interfacial tension than tap water at low temperature. However, their capability of reducing interfacial tension is weakened by heat. Ionic liquid solution and Al_2O_3 nanofluid even resulted in higher interfacial tension than tap water at temperature higher than $50^\circ C$. This phenomenon is important in evaluating the efficiency of using chemicals during thermal recovery processes.

Table 5. Optimum Chemical Concentration based on Interfacial Tension Results

Chemical type	Chemical name	Concentration, % wt
Base case	Tap Water	
High pH solution	Sodium metaborate ($NaBO_2$)	1.50
Ionic liquid	1-Butyl-2,3-dimethylimidazolium tetrafluoroborate ($BMMIM BF_4$)	1.00
Cationic surfactant	C12TAB	0.75
Nanofluids	Silicon Oxide (SiO_2)	1.00
	Aluminum Oxide (Al_2O_3)	0.75
	Zirconium Oxide (ZrO_2)	1.00

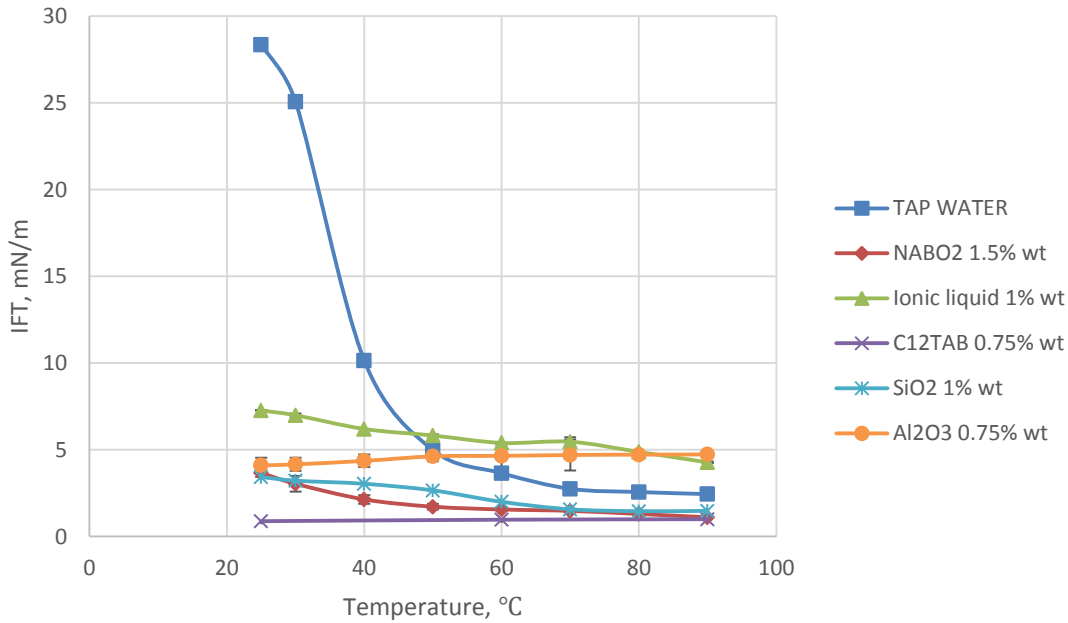


Figure 8. Temperature dependence of IFT in different solution.

2.4.2 Contact Angle. Contact angle measurement is a widely accepted method as a direct indicator of wettability. In this work, contact angle refers to the angle between the solid surface and the tangent line of an oil droplet in the aqueous phase. Contact angle larger than 90° indicates an oil-wet state, while a value less than 90° means water-wetness.

All substrates were treated with heavy oil to establish their oil-wet state before measurement. **Figure 9** shows the wettability of different substrates in this heavy oil and tap water system. Calcite and Indiana limestone were strongly oil wet at 25 to 200°C , while Berea sandstone substrates exhibit intermediate wetness after treatment. The contact angle of mica plate increased when temperature increased from 25 to 90°C , then remained around 135° till 200°C , which is a strong oil-wet state.

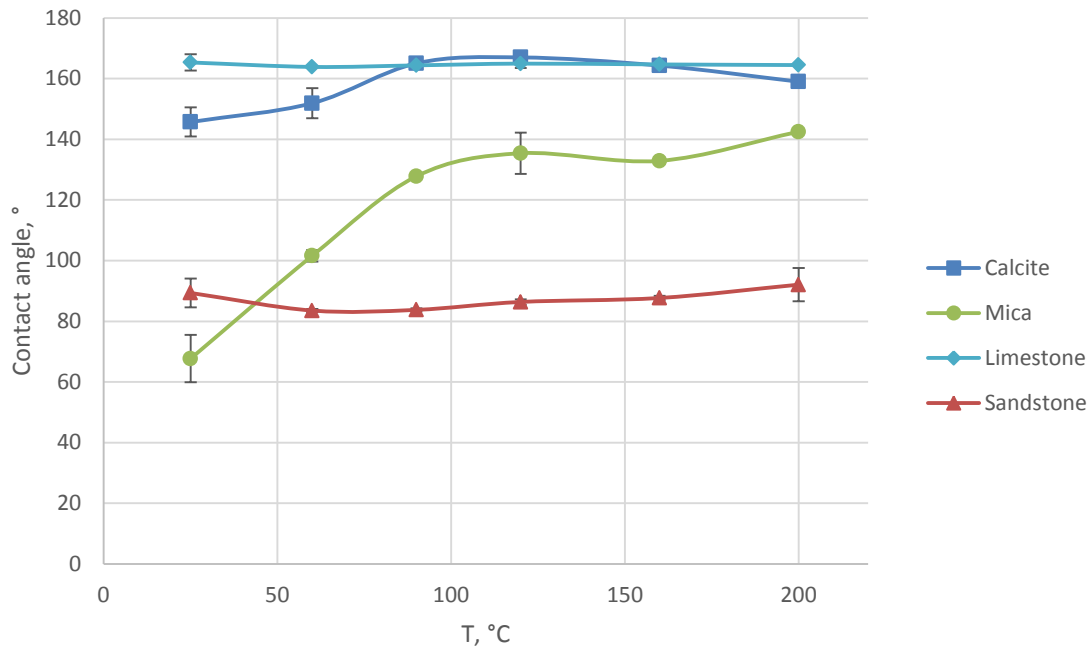


Figure 9. Contact angle results in tap water.

Figure 10 and **Figure 11** show the contact angle in different chemical solution on calcite plate and Indiana limestone, respectively. A few data points for Al_2O_3 and C12TAB at higher temperatures were missing because oil drop spread beyond the range of the camera. For those cases, we assumed the surface tendered strongly oil-wet. It is evident that all five chemical solutions can decrease contact angle on both calcite and limestone at a temperature lower than 120°C , but sodium metaborate and ionic liquid have a better performance than others at a higher

temperature. The capability of wettability alteration of sodium metaborate can be related to the effect of pH on surface charges of carbonate rocks. It was reported in earlier studies (Mohammed and Babadagli 2015b; Zhang and Nguyen et al. 2008) that higher pH reduces the positive charges on calcite surface, thus reducing the adsorption of organic components in oil. Ionic liquid is proven to reduce the adhesion forces between bitumen and sand by about an order smaller because of the formation of ion/charge layers formed on the top of surface (Hogshead et al. 2011).

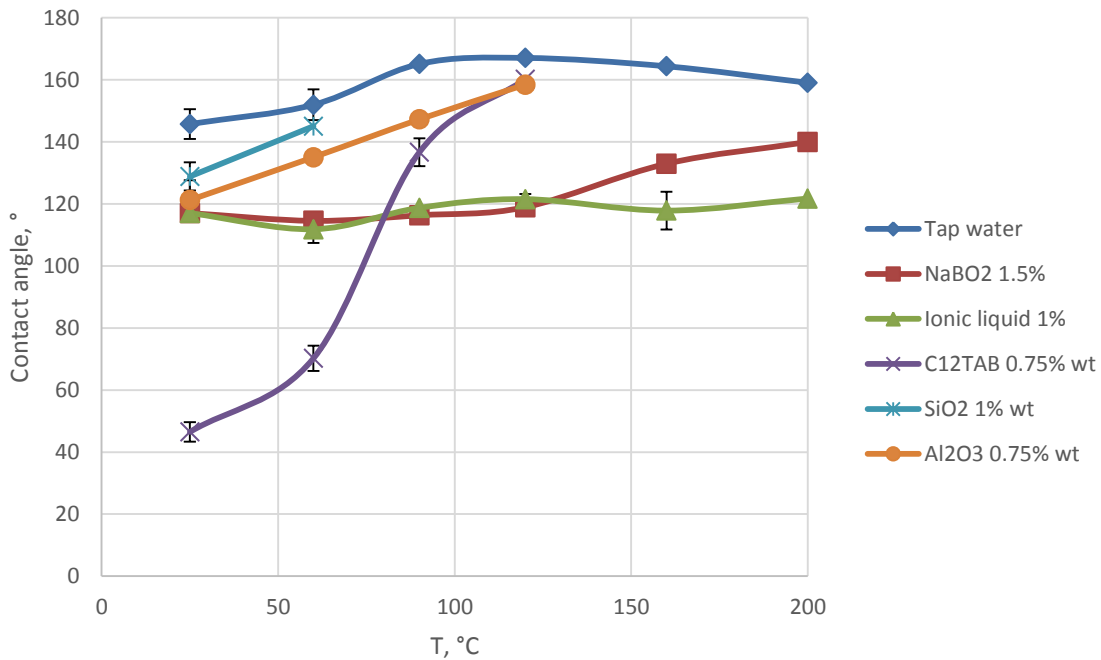


Figure 10. Contact angle results on calcite.

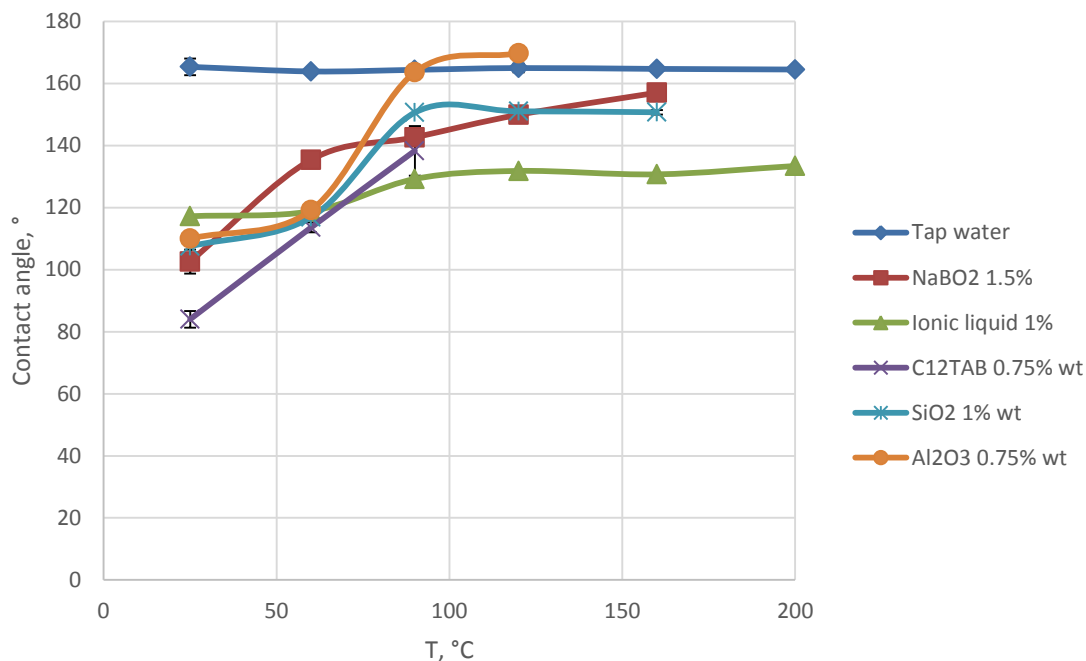


Figure 11. Contact angle results on Indiana limestone.

For mica plates (**Figure 12**) and Berea sandstone substrates (**Figure 13**), sodium metaborate, ionic liquid, and silicon oxide were more efficient in enhancing the oil wetness of surfaces. The mechanism of wettability alteration induced by nanoparticles is not clear yet. Many researchers attempted to relate it to the high surface energy property of nanoparticles and its adsorption on three phase contact region (Wasan and Nikolov 2003; Karimi et al. 2012). One interesting observation is that aluminum oxide, which can significantly reduce contact angle on mica, made sandstone more oil-wet. Considering the heterogeneity of rock sample, the results on mica plate were more reliable and are used in the analyses of the results in the later sections.

C12TBA showed the same trend on all four kinds of substrates. Contact angle in C12TAB solution was much lower than in tap water at 25°C. However, it sharply increased with the increase of temperature. This consists with the trend of interfacial tension (**Figure 7b**). A similar phenomenon was observed in a previous work (Cao et al. 2015) and was attributed to thermal instability.

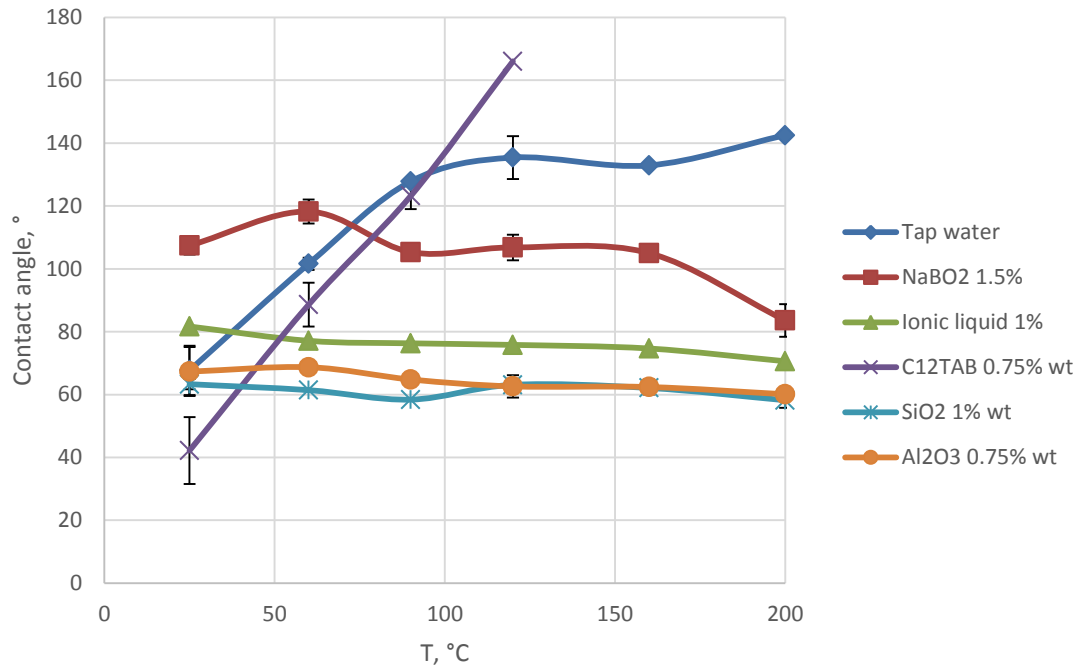


Figure 12. Contact angle results on mica.

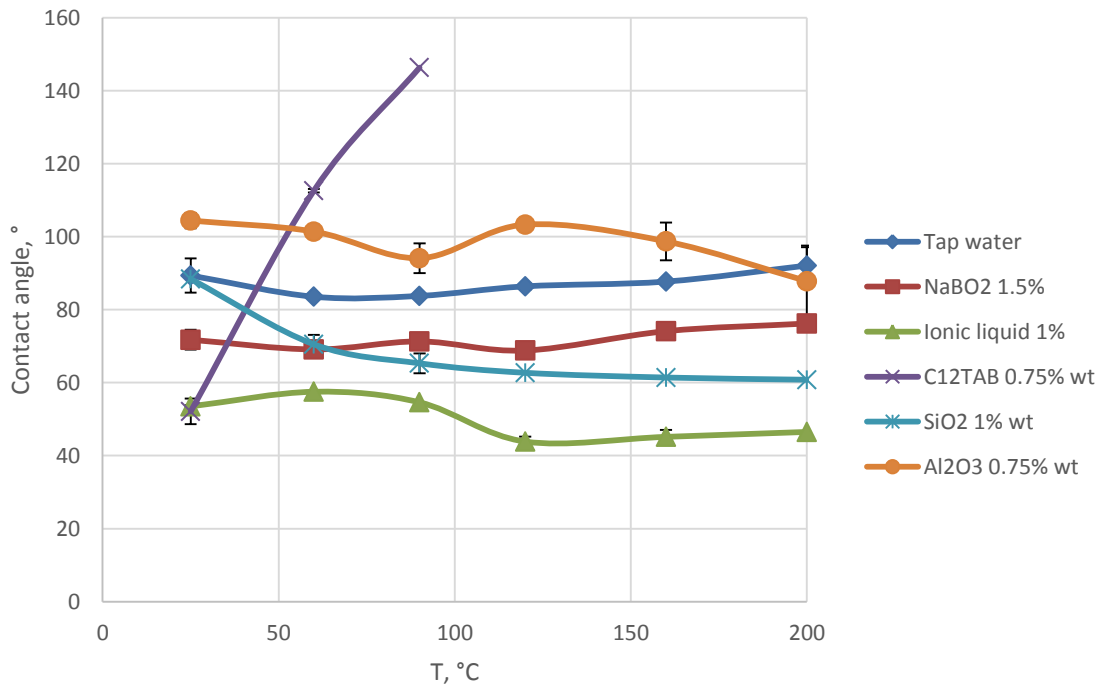


Figure 13. Contact angle results on Berea sandstone.

The capillary (pressure) force is an important factor in evaluating recovery process. Capillary force for simplified tube model can be calculated by:

$$F_c = \frac{2\sigma \cdot \cos\theta}{r} \quad (1)$$

Here the radius of the tube (r) is assumed to be unchanged. Then capillary force is controlled by the combination of surface wettability and interfacial tension. In water-wet cores, θ is smaller than 90° , capillary is the motivation of water imbibition, and oil is expelled in a counter-current fashion. Low capillary force is favorable for enhancing oil recovery. While in oil-wet cores, θ larger than 90° , so capillary is the resistance force. Lower capillary force is expected to give rise to gravity force.

The comprehensive effect of different chemical agents and temperature on the capillary force is shown in **Figure 14**. It can be seen that one chemical agent can have contradicting effects on the capillary force at a different temperature. As shown in **Figure 14a**, the capillary force in C12TAB solution in sandstone at 25°C is positive and higher than in tap water. However, when the temperature increases to 60°C , capillary force turns to negative because of oil wetness. Moreover, SiO_2 nanoparticle, which can reduce the capillary pressure at room temperature, leads to higher capillary force at 90°C ; the same applies to Indiana limestone (**Figure 14b**). At 25°C , all chemical agents can reduce capillary force, especially C12TAB; but when temperature increases, their advantages become less significant.

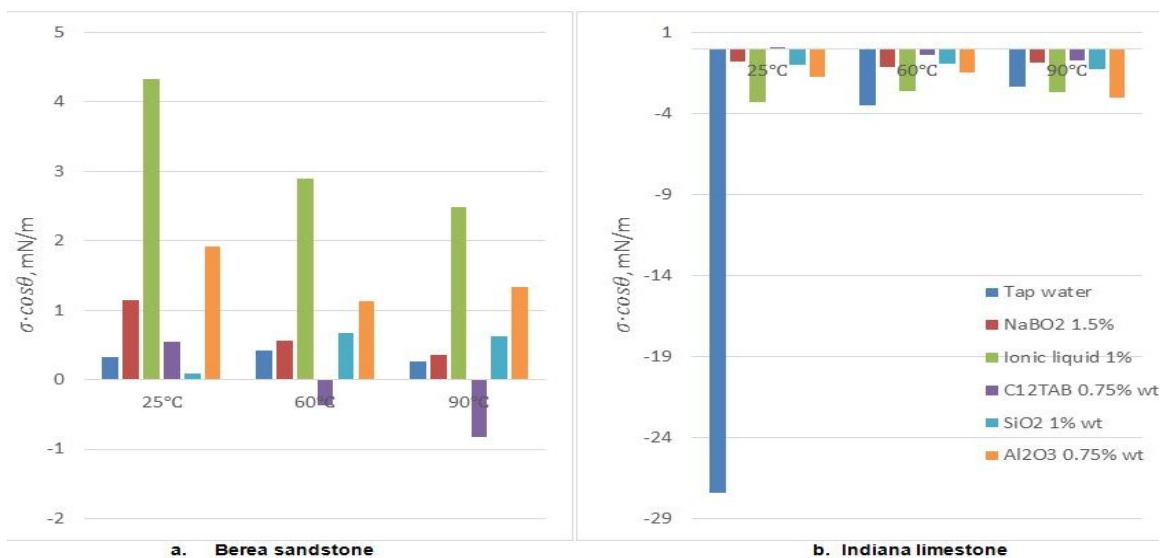


Figure 14. Comprehensive effect of different chemical agents and temperature on capillary force.

2.4.3 AFM Test. To study the mechanism of wettability alteration at the nano-scale, mica and calcite surfaces were scanned before and after the treatment with different chemical solutions. The difference in topography indicates the changes in surface height and composition. Roughness parameters, including average surface height (R_a), root mean square roughness (R_q), maximum surface roughness (R_{max}), and density of peaks (P_{ds}) were calculated to evaluate the alteration quantitatively. Parameters of surface roughness for mica surfaces and calcite surfaces are summarized in **Table 6** and **Table 7** respectively.

Table 6. Surface Roughness Parameters of Different Mica Surface

Substrate	R_a, nm	R_q, nm	R_{max}, nm	$P_{ds}, \mu m^{-2}$
Aged mica	90.8	143	959	0.06
Treated with tap water	16.9	26.9	271	1.01
Treated with $NaBO_2$ solution	0.513	1.22	38.4	0.91
Treated with ionic liquid solution	4.88	9.92	122	0.51
Treated with C12TAB solution	71.9	102	805	0.0178
Treated with SiO_2 nanofluid	1.21	2.48	46.8	3.28
Treated with Al_2O_3 nanofluid	16	21.2	166	5.53
Treated with ZrO_2 nanofluid	15.6	29.1	297	3.66

Figure 15 presents the topography of coated mica. Oil droplets with a comet-like shape randomly adsorbed on the mica surface. The oil shape was caused by centrifuge process and the trail points to the outside direction of the centrifuge. The special comet shape of oil droplet was used to distinguish oil from other adsorbed components.

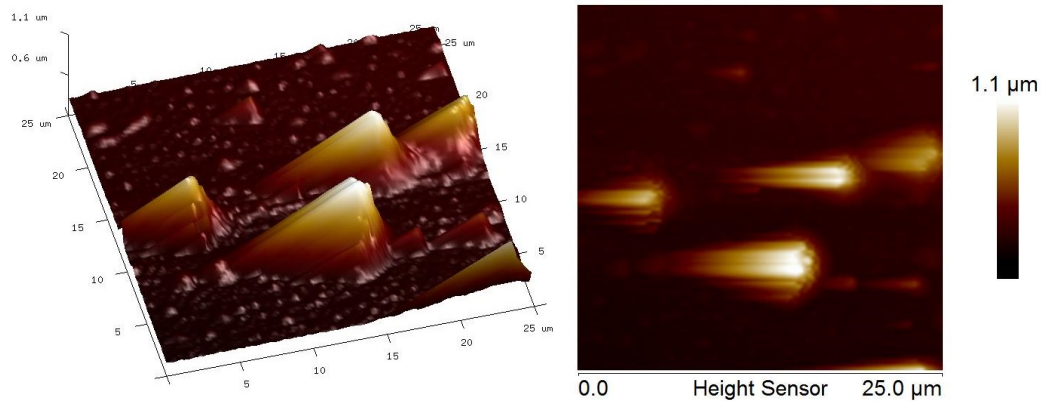


Figure 15. 2D and 3D topography image of aged mica.

Figure 16 is the surface image of the mica sample that was soaked in tap water at 90°C for 20 hours. Compared with Figure 15, one may observe that the oil droplets were separated into a smaller size; however, they were still adsorbed on the surface. This is verified by the change of roughness parameters in Table 6. Average surface height decreased from 90.8 nm to 16.9 nm, while peak density increased from $0.06 \mu\text{m}^{-2}$ to $1.01 \mu\text{m}^{-2}$. Oil adsorption became more uniform and a larger proportion of the surface was coated by oil. This observation consists with the contact angle result in Figure 12 where mica surface changed from water-wet to oil-wet in tap water when temperature increased from 25°C to 90°C.

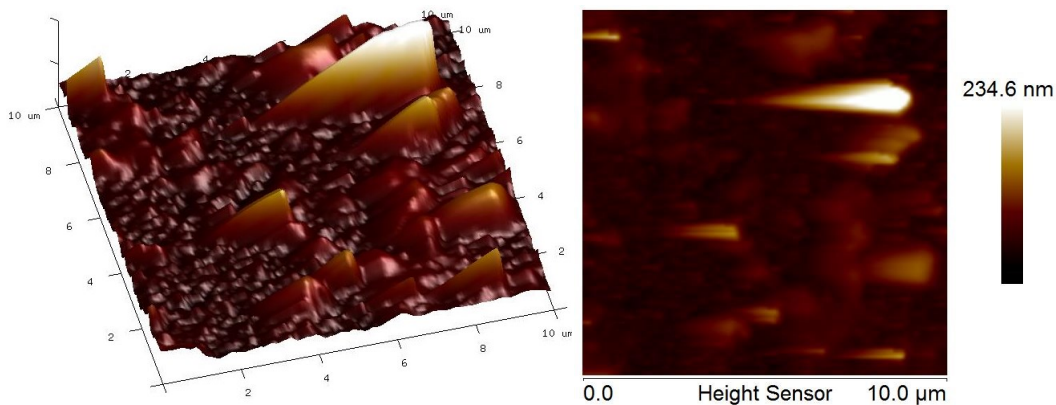


Figure 16. 2D and 3D topography image of mica sample treated with tap water at 90°C for 20 hours.

After being soaked in NaBO_2 solution for 20 hours, most oil droplets were removed (**Figure 17**) and the average roughness dramatically decreased to 0.513 nm. This means the surface properties is more controlled by the original properties of fresh mica. Combined with the contact angle results in Figure 12, the capability of NaBO_2 to alter wettability of mica can be attributed to its ability to removed adsorbed oil components on the surface.

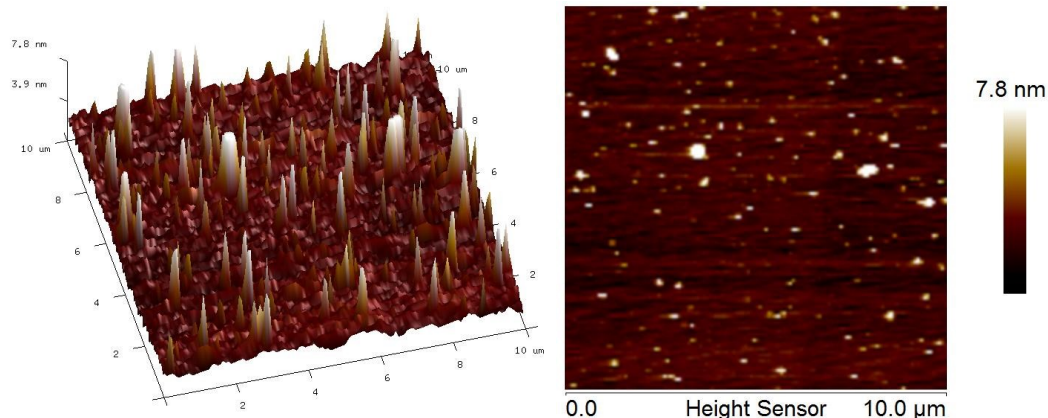


Figure 17. 2D and 3D topography image of mica sample treated with $NaBO_2$ solution at $90^\circ C$ for 20 hours.

The surface image of mica sample treated with ionic liquid is shown in **Figure 18**. It is obvious that the surface was cleaner than the sample that was only treated with only tap water (Figure 16). Also, the regular circle shape of most peaks on this sample indicates that they are not oil droplets. It is reasonable to speculate that most of them are adsorbed $BMMIM BF_4$ molecular. This speculation consists with the theory suggested by previous studies that ionic liquid molecular can adhere to the surface by forming an oil/charge layer that alter surface properties (Wasserscheid and Keim 2000; Hogshead et al. 2011).

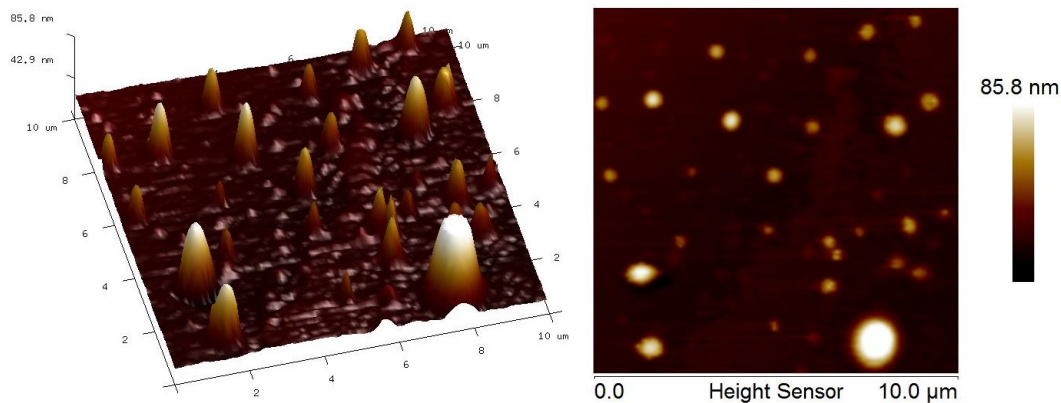


Figure 18. 2D and 3D topography image of mica sample treated with ionic liquid solution at $90^\circ C$ for 20 hours.

The sample shown in **Figure 19** was soaked in C12TAB solution at $90^\circ C$ and has the smoothest surface among all seven scanned samples. As shown in Table 6, the peaks density is as low as $0.0178 \mu m^{-2}$. However, the average surface height is 71.9 nm , which is higher than the average

height of sample treated with tap water. So, even though there were less peaks and valleys on the surface, the high R_a value indicates that a smooth and continuous oil film was formed on the top of mica surface. This explanation consists with oil-wet state of mica in C12TAB solution (Figure 12).

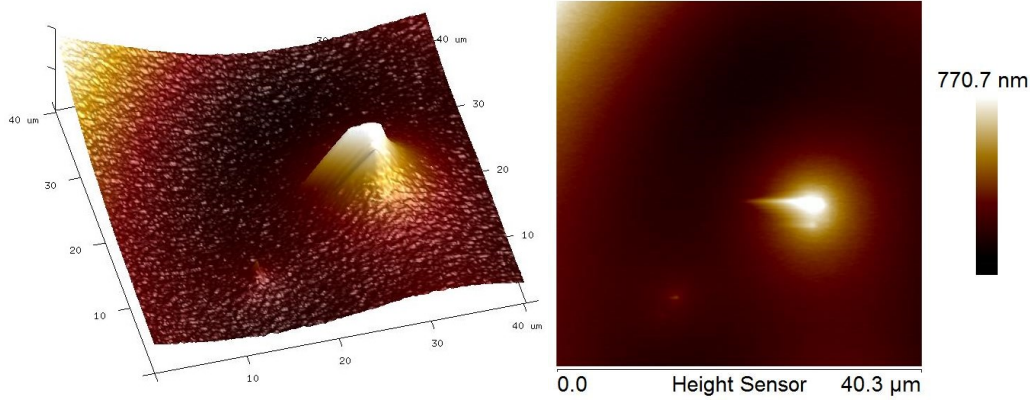


Figure 19. 2D and 3D topography image of mica sample treated with C12TAB solution at 90°C for 20 hours.

Among three mica samples that were treated with different nanofluids, the sample in SiO_2 nanofluids has the smallest average roughness and peaks density (Table 6). This indicates that SiO_2 nanoparticles have the best capability to remove oil in three tested nanoparticles. By comparing Figure 12 with **Figure 20**, it can be seen that after being soaking in SiO_2 nanofluid, most adsorbed oil was removed and more mica surface was exposed. The observation in AFM test consists with the wettability results. As shown in Figure 12, contact angle measured on mica surface was only 61.4° in SiO_2 nanofluids.

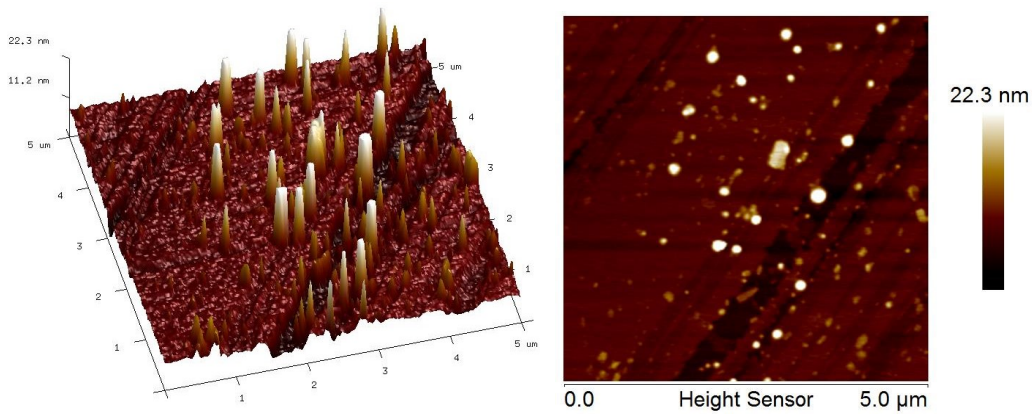


Figure 20. 2D and 3D topography image of mica sample treated with SiO_2 nanofluid at 90°C for 20 hours.

Figure 21 shows that after being soaked in Al_2O_3 nanofluid, mica was covered with a smaller-sized oil droplet. Average roughness, maximum roughness decreased, while peak density increased from $0.06 \mu\text{m}^{-2}$ to $5.53 \mu\text{m}^{-2}$. The change in Al_2O_3 nanofluid is similar to the process with tap water in that there was separation of big oil drops. Big oil drops were separated into smaller oil droplets but were not removed from the surface. So, no obvious improvement of the wettability was observed in Al_2O_3 nanofluid.

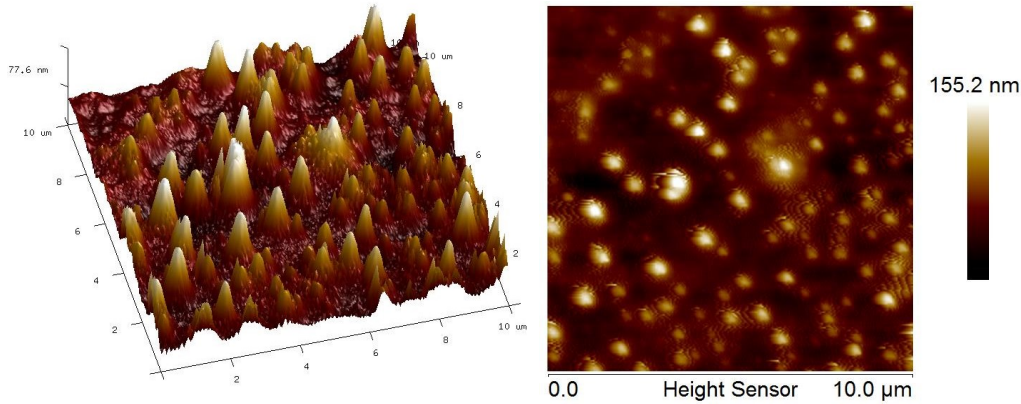


Figure 21. 2D and 3D topography image of mica sample treated with Al_2O_3 nanofluid at 90°C for 20 hours.

The sample that was treated with ZrO_2 nanofluid had the biggest peaks density among all scanned samples (Table 6). However, only 3.83% of total peaks had a height larger than 55 nm. Also, as shown in **Figure 22**, only a minority of the peaks had a comet-like shape, while the others had small circle dots, which could be ZrO_2 nanoparticles. So, the mechanism of wettability alteration caused by ZrO_2 nanofluid is expected to be related to the adsorption of ZrO_2 nanoparticles and removal of oil droplets.

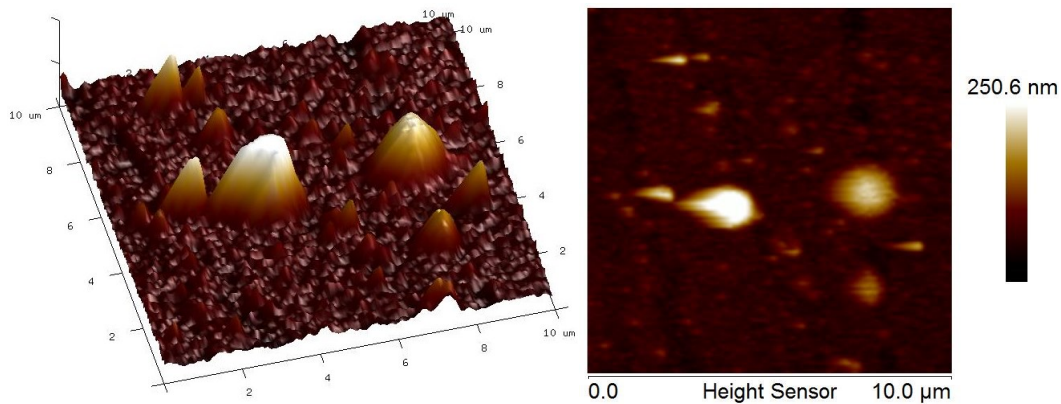


Figure 22. 2D and 3D topography image of mica sample treated with ZrO_2 nanofluid at 90°C for 20 hours.

As shown in **Figure 23**, calcite surface is fully covered with oil after being aged for 5 days. Although R_a and R_{max} for coated calcite (**Table 7**) are smaller than coated mica (Table 6), the oil film on calcite is more uniform. Therefore, coated calcite is more oil-wet than coated mica.

Table 7. Surface Roughness Parameters of Different Calcite Surface

Substrate	R_a, nm	R_q, nm	R_{max}, nm	$P_{ds}, \mu m^{-2}$
Aged mica	17	23	196	0.10
Treated with tap water	7.37	10.9	154	1.00
Treated with $NaBO_2$ solution	1.42	1.79	16.2	0.01
Treated with ionic liquid solution	9.49	16.4	281	11.95
Treated with C12TAB solution	11	15.6	179	2.43
Treated with SiO_2 nanofluid	35.8	45.7	338	0.12
Treated with Al_2O_3 nanofluid	34.9	42.7	309	0.33
Treated with ZrO_2 nanofluid	22.2	28.3	180	0.37

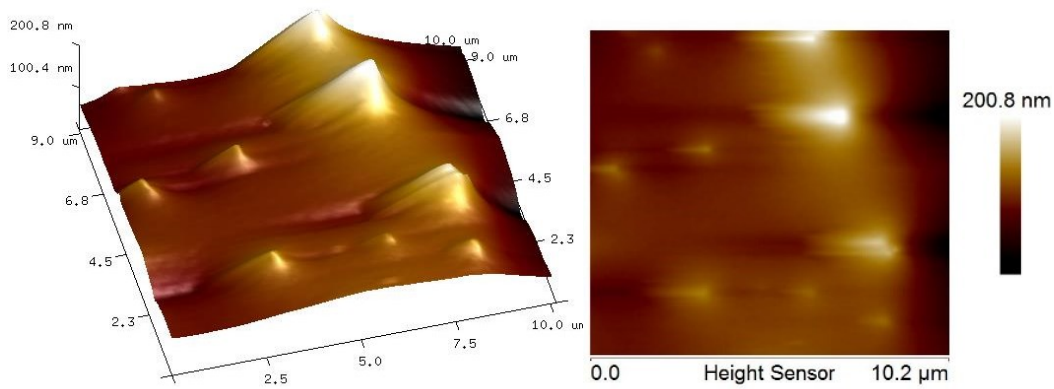


Figure 23. 2D and 3D topography image of aged calcite.

After being soaked in tap water for 20 hours, average roughness and maximum roughness decreased, which indicates the oil film gets thinner. However, from Figure 16 we can see the surface was still completely covered with oil. Therefore, the wettability of calcite was not improved after the treatment, as the contact angle was as high as 165° (Figure 10).

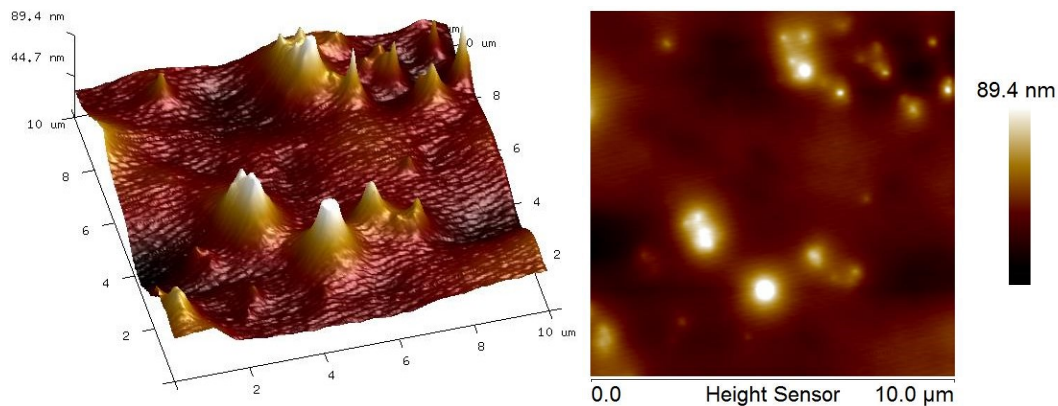


Figure 24. 2D and 3D topography image of calcite sample treated with tap water at 90°C for 20 hours.

The calcite treated with NaBO_2 solution has the weakest R_a , R_q , R_{max} and P_{ds} among all samples. As shown in **Figure 25**, the sample has a clean surface with some small dents. Therefore, NaBO_2 helped to remove the adsorbed oil and the surface properties were dominated by the property of fresh calcite. This observation consists with the reduction of contact angle previously mentioned.

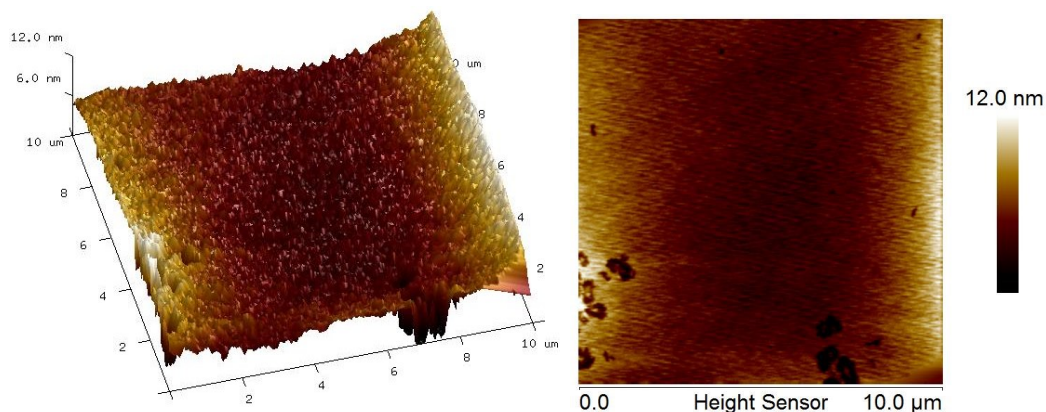


Figure 25. 2D and 3D topography image of calcite sample treated with NaBO_2 solution at 90° C for 20 hours.

As shown in Figure 10, calcite in ionic liquid solution has the similar contact angle with that in NaBO_2 solution, as both reduced the contact angle by 47°. However, they have a different surface in nanoscale. In Table 7, the sample treated with ionic liquid has the biggest peak density, which indicates the most dispersive adsorption of small oil drop (**Figure 26**). The adsorption of BMMIM BF_4 molecule on mica surface (Figure 18) was not observed in the test with calcite.

Therefore, the mechanism of wettability improvement in the ionic liquid is that it helps with breaking oil film and the removal of oil bulk.

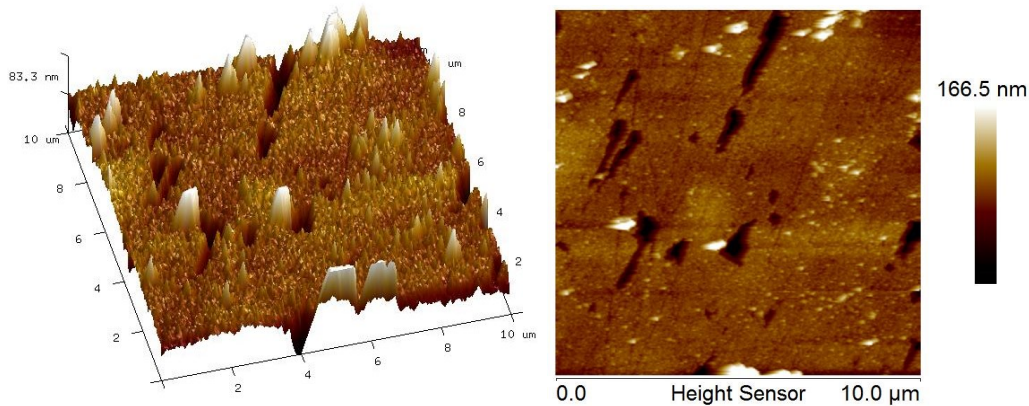


Figure 26. 2D and 3D topography image of calcite sample treated with ionic liquid solution at 90° for 20 hours.

In **Figure 27**, the calcite sample treated with the C12TAB solution is covered with oil droplet of varying sizes. Peak density is as high as $2.43 \mu\text{m}^{-2}$, which indicates the original oil film (Figure 23) was broken but not removed. Therefore, the improvement of wettability in C12TAB is very limited.

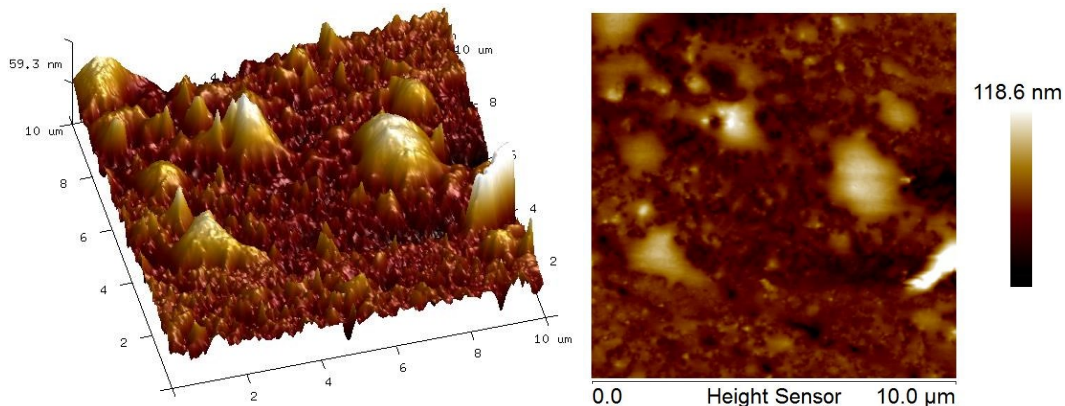


Figure 27. 2D and 3D topography image of calcite sample treated with C12TAB solution at 90°C for 20 hours.

The contact angle for the calcite in SiO_2 at 90°C was not included in Figure 10 because of oil spreading out of the lens coverage before reaching equilibrium. However, the results from AFM confirm the strong oil wetness of that surface. As shown in Table 7, this sample has the biggest average roughness and maximum roughness. In **Figure 28**, the surface was completely covered

with a thick oil film, which is similar to the surface condition of the aged calcite sample (Figure 23). The difference between Figure 20 and Figure 28 explains why SiO_2 nanoparticles can significantly reduce contact angle on mica while impairing on calcite.

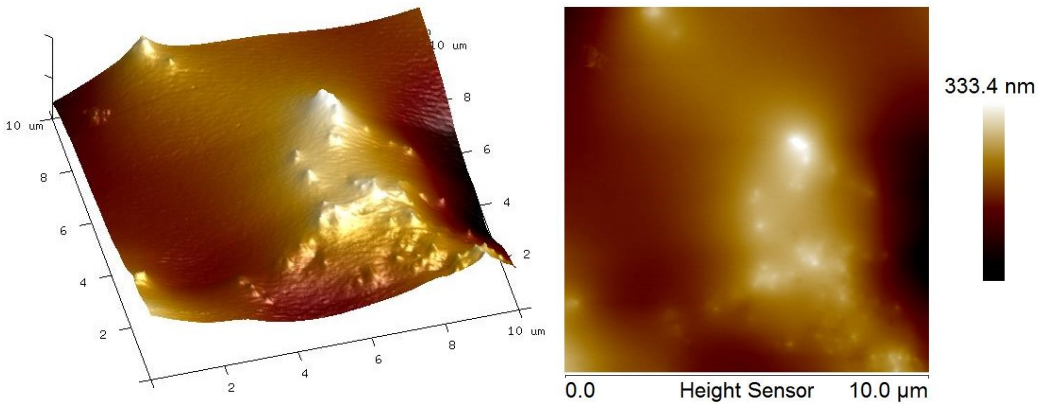


Figure 28. 2D and 3D topography image of calcite sample treated with SiO_2 nanofluid at 90°C for 20 hours.

The calcite surface soaked in Al_2O_3 nanofluid was covered by an oil film with a saw-tooth wave-shape (**Figure 29**). There are ‘water ripples’ on the wave surface. The formation of the wave pattern is not clear yet.

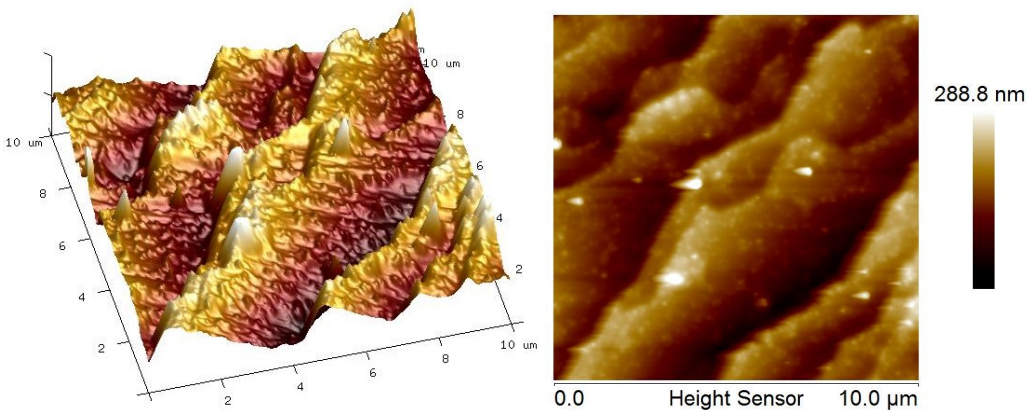


Figure 29. 2D and 3D topography image of calcite sample treated with Al_2O_3 nanofluid at 90°C for 20 hours.

In **Figure 30**, we can see the oil film on calcite surface had more humps after being soaked in ZrO_2 nanofluid for 20 hours. As indicated in Table 7, peak density increased from $0.1\mu\text{m}^{-2}$ to $0.37\mu\text{m}^{-2}$ after the treatment. According to the surface image, however, the wettability of calcite

surface cannot be improved by ZrO_2 nanoparticles. Considering its strong performance in imbibition test (**Figure 31**), ZrO_2 is speculated to enhance recovery by reducing interfacial tension rather than contact angle.

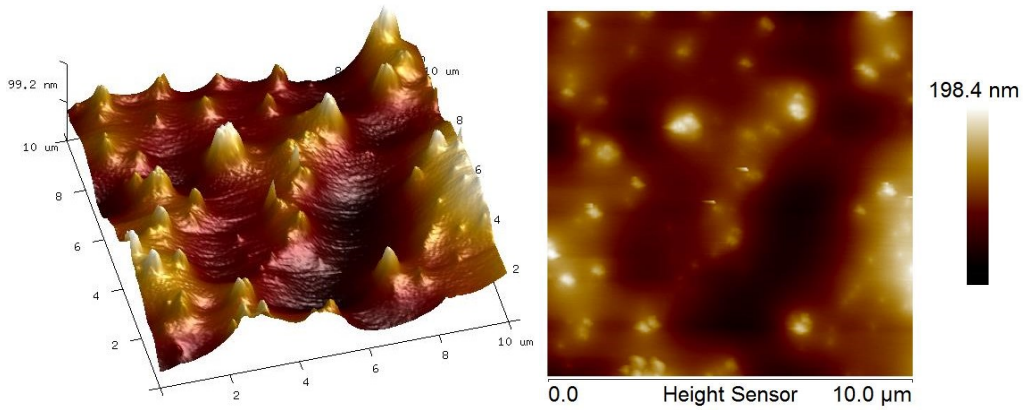


Figure 30. 2D and 3D topography image of calcite sample treated with ZrO_2 nanofluid at 90°C for 20 hours.

2.4.4 Capillary Imbibition. Indiana limestone was soaked into chemical solutions at 90°C and ambient pressure. Oil recovery from each core was recorded continuously for 100 days. **Figure 31** gives oil recovery from limestone cores versus time in different chemical solution. After being soaked in tap water for 100 days, only 29.83% PV oil was recovered because of strong oil wetness.

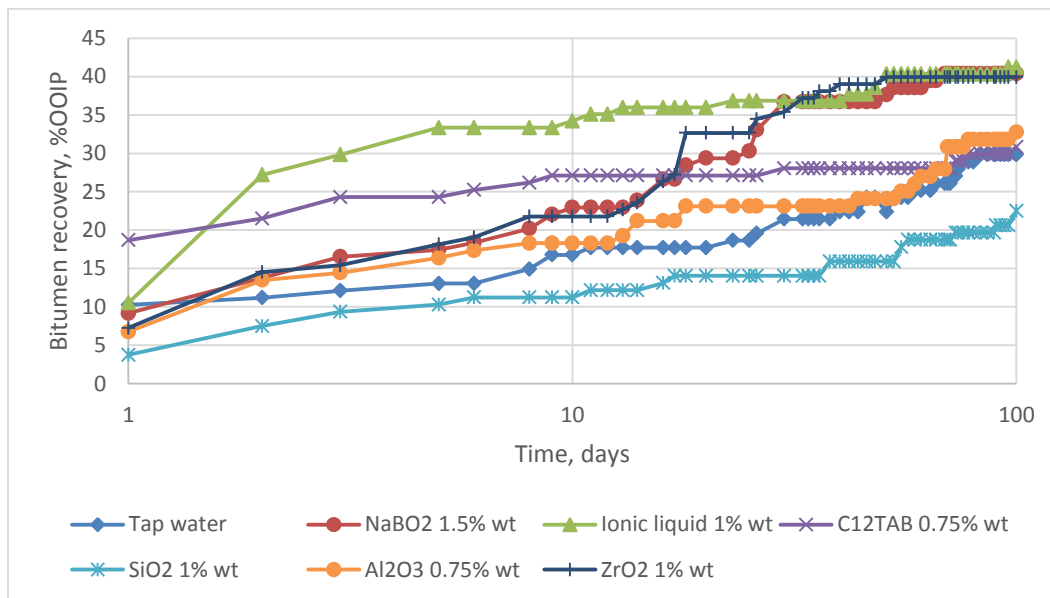


Figure 31. Oil recovery vs. time in limestone cores at 90°C.

It can be seen that ionic liquid had the best performance among all chemical agents. Oil recovery in ionic liquid was increased to 41.23% PV after 100 days. Considering higher interfacial tension than all other solution, the high efficiency of ionic liquid is contributed to its capability of improving the surface wettability of limestone. As shown in **Figure 32a**, limestone substrates in ionic liquid had the lowest contact angle, which means the most water-wet state, among all six tested solutions.

ZrO_2 nanoparticles and $NaBO_2$ also exhibited a great capability to increase oil recovery. Both produced about 40% PV oil by the end of 100 days and their recovery curves are similar. In Figure 32a, $NaBO_2$ increases production by reducing both contact angle and interfacial tension. However, the interface properties in ZrO_2 nanofluid were not measured in this study because it is not transparent and cannot be observed with our IFT device.

The core in C12TAB had a similar final recovery factor with the core in tap water. Both of them ended producing about 30% PV in 100 days, but the former produced about twice amount oil in the first day. When soaked in C12TAB solution, more than 18% PV oil was expelled in only one day, which is 60.62% of the final production. The high recovery rate at the beginning of the test is related to the thermal instability of C12TAB. As shown in the previous section, C12TAB solution can change the wettability of calcite to water-wet at temperature lower than 70°C . Thus, spontaneous imbibition occurred during heating. After temperature increased to 90°C , the capability of C12TAB was weakened. Therefore, spontaneous imbibition stopped and oil recovery rate slowed down.

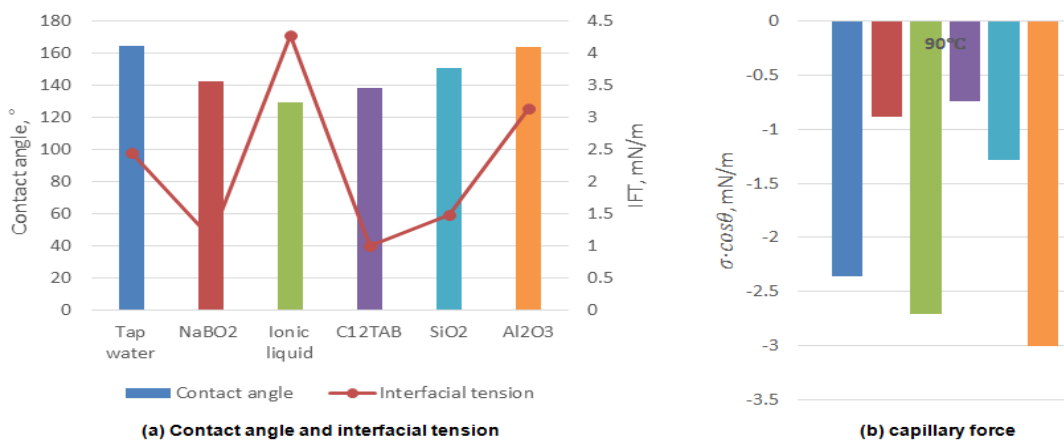


Figure 32. Surface properties and capillary force for limestone at 90°C .

The behaviour of Al_2O_3 and SiO_2 in imbibition was not compatible with contact angle and interfacial tension results. Interfacial tension measured in SiO_2 nanofluid was only half of that in Al_2O_3 nanofluid. But Al_2O_3 nanofluid expelled more oil than in SiO_2 . This abnormal observation is related to the inaccuracy of concentration, which is caused by instability of Al_2O_3 nanoparticles in water (**Figure 33**). On the one hand, as discussed in the previous section, the interfacial tension and contact angle were measured with Al_2O_3 concentration lower than 0.75%wt. On the other, after Al_2O_3 nanoparticle settled down in imbibition cell, the actual Al_2O_3 nanofluid that was imbibed into the core was higher than 0.75%wt. Hence, it is reasonable to believe that Al_2O_3 nanofluid with higher concentration can further improve surface properties.



Figure 33. Nanofluids are unstable at 90°C (left: SiO_2 , middle: Al_2O_3 ; right: ZrO_2).

The same chemicals in capillary imbibition tests after exposing the sample to solvent for 10 days at room temperature were used in a previous study (Mohammed and Babadagli 2014). These results are compared with our results at 90°C in **Figure 34**. The performance of water is remarkably higher at the higher temperature despite the pre-solvent treatment of the sample in the previous study experiments (Mohammed and Babadagli 2014). The difference in the recovery is beyond the capability of thermal expansion indicating that the temperature improved the capillary imbibition and gravity drainage due to the reduction in oil viscosity and interfacial tension at the higher temperature. The difference in the recovery at 90°C and 25°C in C12TAB was less than the difference in other chemical solutions as the capability of C12TAB in enhancing oil production was impaired by heat because of thermal instability. More interestingly, the core soaked in Al_2O_3 nanofluid produced only 1% oil at 25°C, which was less than the oil

expelled from the distilled water. Its performance at the higher temperature is quite significant indicating an improvement in capillary imbibition and gravity drainage caused by strong wettability alteration. The same comment can be made for ZrO_2 . Ionic liquid showed the best performance at the higher temperature even though its recovery was less than C12TAB at the room temperature. This comparative plot given in Figure 34 indicates the thermal stability of these three chemicals (ionic liquid, ZrO_2 , Al_2O_3) at high temperatures as well as their applicability at elevated temperatures.

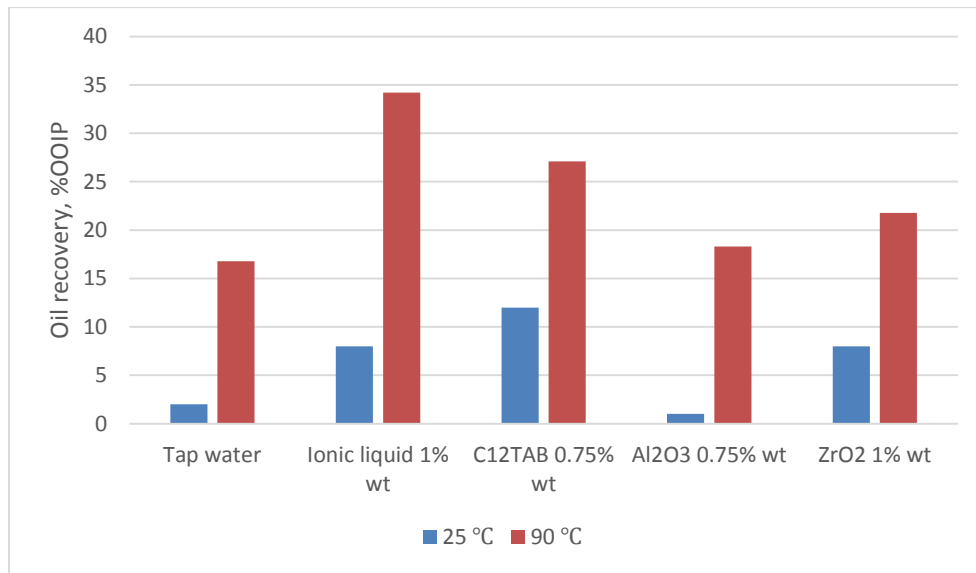


Figure 34. Comparison of production in 10 days at 25°C (Mohammed and Babadagli 2014) and 90°C.

Sandstone cores were tested in the same chemical solutions at 90°C and ambient pressure. The volume of oil expelled from cores was recorded for 100 days. Compared with the production of Indiana sandstone, the recovery factor of Berea sandstone was higher because it is more water-wet. After 100 days, 47% OOIP was expelled by water (**Figure 35**).

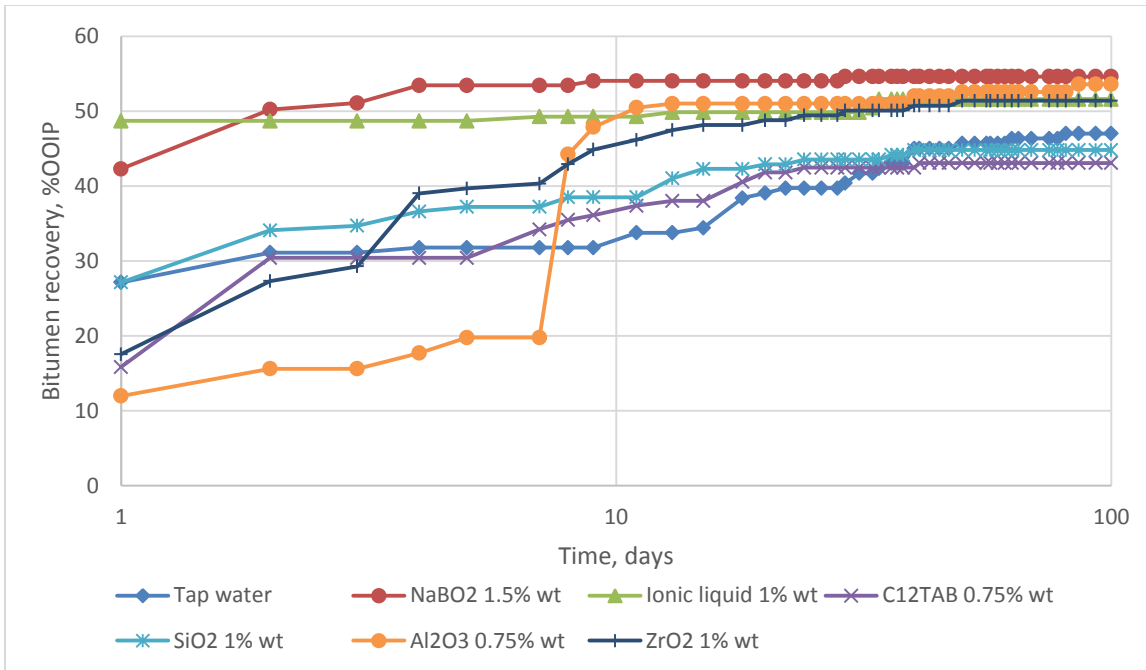


Figure 35. Oil recovery vs. time in sandstone cores at 35°C.

The best performance was observed in the core in NaBO₂ solution. The ultimate recovery factor was as high as 54.67%. This high production can be attributed to relatively small contact angle in the oil/sandstone/ NaBO₂ solution system (**Figure 36a**). Although the oil recovery in Al₂O₃ nanofluid was similar to recovery in NaBO₂ solution, recovery rate was quite different. 42.31% OOIP was produced from the core in NaBO₂ solution in the first day, while only 11.98% OOIP came out in Al₂O₃ nanofluid in the same amount of time. Another interesting observation about the production in Al₂O₃ nanofluid is the dramatic jump in production at 7 (19.78%) to 8 days (44.26%). Figure 36a shows the interfacial properties measured in these two chemicals were similar; therefore, the big difference could be related to the instability of Al₂O₃ nanofluid (Figure 33). One possible reason for this is that as Al₂O₃ nanoparticles settled down as the cloud at the bottom of the cell, produced oil was held at the bottom rather than raising to the up-scaled part of the cell in the first 7 days.

Ionic liquid also increased oil recovery as 51.62% OOIP was recorded by the end of 100 days. Also, the production rate was fastest among all tests. 47.73% OOIP came out of the core on the first day, which was 92.46% of the final production. The high recovery rate is contributed to the strong capillary force. Ionic liquid gave the biggest interfacial tension and smallest contact angle

(Figure 36a), leading to the highest positive capillary force (Figure 36b), which means the strongest driving force.

The production in SiO_2 nanofluid reached equilibrium after 40 days and 44.83% PV was recorded as ultimate recovery, which is a little bit lower than the final production with tap water (Figure 35). Although SiO_2 nanoparticle can reduce both contact angle and interfacial tension, the effect is not significant enough to increase production (Figure 36a). Among all test chemicals, C12TAB had the worst performance as only 43% OOIP was expelled in 100 days. The production was impaired because sandstone is oil-wet in C12TAB solution at 90°C (Figure 36a). The capillary force is the resistance force and oil can only be expelled out when it is overcome by gravity force.

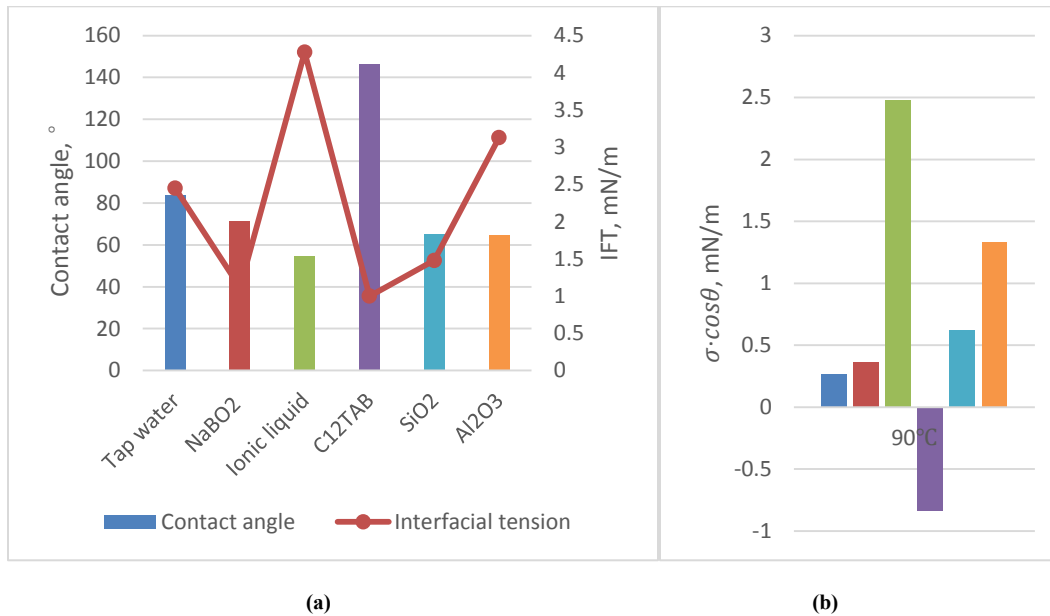


Figure 36. Surface properties and capillary force for sandstone at 90°C: (a) Contact angle and interfacial tension; (b) capillary force.

2.5 Conclusions

“New generation” wettability alteration chemicals were tested for heavy oil- recovery from sandstone and carbonate rock types at elevated temperatures. The partial effect of those chemical agents on altering wettability and interfacial tension was clarified through contact angle and interfacial tension measurements supported by spontaneous imbibition tests. The mechanism of wettability alteration was studied with AFM tests. All chemical agents significantly reduced the

interfacial tension at low temperatures. However, their capability was weakened as temperature was increased. The same trend applied to the contact angle on limestone samples and mica.

$NaBO_2$ exhibited good thermal stability in wettability alteration and interfacial tension reduction. It also improved imbibition spontaneous in the limestone case by reducing negative capillary force, thus giving rise to the gravity force.

Ionic liquid had the best performance in this heavy oil/limestone system. The high efficiency was owing to the capability of reducing oil wetness of limestone by removing adsorbed oil on the rock surface.

Contact angle and interfacial tension in C12TAB solution increased with temperature. Although oil recovery from limestone was high in imbibition test, it is not a good choice for thermal recovery in carbonates.

Silicon oxide nanoparticle was more efficient in reducing interfacial tension than aluminum oxide. It was also more thermally stable than aluminum oxide.

Zirconium oxide nanoparticle is promising in enhancing oil recovery from carbonate. A more detailed study is needed on the surface properties of heavy oil/rock system for this chemical, which is the on-going part of the research.

Chapter 3: Selection of New Generation Chemicals as Steam Additive for Cost Effective Heavy-Oil Recovery Applications

This chapter is an improved version of paper SPE 184975, which was presented SPE Canada Heavy Oil Technical Conference held in Calgary, Alberta, Canada, 15—16 February 2017. A version of this paper has been submitted to SPE Reservoir Evaluation and Engineering Journal for publication.

3.1 Preface

One of the ways to improve the efficiency of steam injection is to use chemicals as an additive to alter interfacial properties. Historically, this has been tested using surfactants, which are expensive and thermally unstable. Therefore, commercial applications have been highly limited in that area over the past three decades. In conjunction with recent efforts using new generation materials as EOR agents, we performed a screening study to identify the potential chemicals/materials for heavy-oil recovery and to investigate the applicability of selected new generation chemicals as interfacial properties modifiers at steam temperature.

Different experimental methods, including capillary imbibition tests, i.e. contact angle and interfacial tension measurements, were combined to understand the mechanism of alteration surface interplay (wettability and interfacial tension) using different chemical agents. Capillary imbibition tests were conducted to study the potential of these chemicals to alter wettability and rock/chemical interactions on aged limestone and sandstone cores at high temperature. Pendant drop interfacial tension (IFT) and contact angle measurements were performed using a high pressure and high-temperature cell under the same -steam- conditions.

Seven different chemical agents including a high pH solution (sodium metaborate), an ionic liquid, a cationic and an internal olefin sulfonate (IOS) surfactant, and nanofluids (silicon, aluminum and zirconium oxides) were tested in this study. Indiana limestone and Berea sandstone samples were saturated and aged in heavy oil with a viscosity of 6,000 cp. Capillary imbibition tests were conducted under high temperature (between 90°C and 180°C) and high pressure (185 psi) conditions using a newly-manufactured visual cell. The production rate and ultimate recovery were used to evaluate the capability of different chemicals changing the interfacial properties and their thermal stability at steam temperature. Contact angles between heavy oil and mica/calcite plates were measured under the same conditions. Finally, the stability of the chemicals was measured through thermal gravimetric analysis (TGA). The combination of all these results helped to identify the applicability of the selected chemicals under steam conditions for carbonates. Technical and economic limitations for each chemical as well as the way the chemical contributes to recovery (wettability alteration or IFT reduction) were identified.

Investigation of interfacial properties alteration induced by new generation chemicals at high temperature is helpful in the selection and application of efficient and economical chemicals in steam based heavy-oil recovery methods.

Key words: New generation chemicals, steam conditions, alteration of interfacial properties, wettability alteration for carbonates and sandstones.

3.2 Introduction

Because of continuous decline of conventional oil reserves, more attention has been devoted to the exploitation of heavy oil reservoirs. Thermal recovery has historically been the primary technique to improve the recovery from this type of reservoir. By injecting heat into the reservoir, oil viscosity could be greatly reduced yielding a significant improvement in recovery factor. However, for oil-wet carbonate reservoir containing heavy or extra-heavy oil, the effectiveness and economy of thermal recovery are limited by the adverse interfacial properties in oil/water (steam)/rock system. Hence, adding chemical agents to injected hot water or steam has been put forward and widely studied in the laboratory. Early attempts mainly focused on combining thermal recovery with solvent injection (Frauenfeld et al. 2007; Sharma and Gates 2013) and surfactant flooding (Green and Malcolm 1985; Handy et al. 1982; Maini and Ma 1985). In recent years, cost effective chemicals that can improve the performance of thermal application has received more attention due to the lower cost and their thermal stability. These chemicals were tested for their ability to alter wettability and interfacial tension.

Wettability is a critical factor that affects the rate and extent of the recovery process. 84% of carbonate reservoirs in the world are suggested to be oil wet (Wang et al. 2011). The efficiency of water or steam injection in those reservoirs is greatly weakened by this unfavorable property, thus making wettability alteration necessary and essential. Wettability alteration generally refers to the process that increases the water wetness of reservoir by thermal or chemical methods (Mohammed and Babadagli 2015). The high temperature was proved to be able to modify the wettability in carbonates by different researches. Carbonates tend to be more water wet at high temperature (Motealleh et al. 2015). Al-Hadhrami and Blunt (2010) concluded there is a critical temperature, which the rock can change from oil-wet to water-wet because of the detachment of

asphaltene. Hamouda and Gomari (2006) further explained the reverse of calcite wettability at increasing temperature with electro-kinetic measurements. The results showed this change is caused by the reduction of positive charge of the surface because of less available Ca^{2+} sites, thus leading to less adsorption of acids on the calcite surface. Hence, theoretically, injecting steam or hot water to a carbonate reservoir can improve wettability and induce capillary imbibition. But considering environmental and economic issues, chemical methods seem to be more practical. Mohammed and Babadagli (2015) reviewed the wettability alteration process in sandstones and carbonates induced by different chemical agents, including surfactants, alkaline-anionic surfactant mixtures, high pH solutions, low salinity water, smart water and nanofluids. The application, limitation and working mechanism of different categories of chemicals were systemically summarized in this work.

Interfacial tension is another important parameter in immiscible displacement. Core flooding results showed that a sufficient reduction in IFT can greatly increase the efficiency of displacement in cores with different wettability conditions (Wagner and Leach 1966). IFT between oil and displacing fluid is mainly affected by pressure, temperature, additives in injected fluid, and the composition of the oil. The effect of temperature on IFT was widely investigated in early studies (Wagner and Leach 1966; Babu et al. 1984). Besides temperature, using chemicals in the aqueous phase to reduce IFT has been the main mechanism of improving production in tertiary recovery. Surfactants are highly efficient in reducing interfacial tension in oil/water system. According to Wade et al. (1977) and Hayes et al. (1979), obtaining an ultralow IFT (lower than 10^{-3} mN/m) is possible at low surfactant concentration.

As promising environmentally-friendly alternates to surfactants, ionic liquids also exhibit the good capability of reducing IFT at low concentration. Hezave et al. (2013) observed IFT values about fifty times lower in ionic liquid ($[C_{12}min][Cl]$) solution at critical micelle concentration. Benzagouta et al. (2013) and Emad (2013) proved the stability of Ammoeng group ionic liquids at temperature up to 90°C and found the IFT between oil and ionic liquid solutions is correlated with temperature.

Alkali is another important additive that can modify surface forces. It is generally accepted that alkalis change the oil/water IFT by reacting with the acidic component in the crude oil to form in-situ soap. The minimum IFT values can be obtained at certain pH ranges (Jeff and Wasan 1993).

LTS-18 belongs to internal olefin sulfonate (IOS) family, which is commercially described as ENORDETTM. IOS has been used in EOR design for many years. Early reports include the use in co-surfactant-enhanced alkaline flooding (Falls et al. 1994) and alcohol-free chemical flooding (Sanz and Pope 1995). The properties, like good thermal stability, high solubility, and low cost, make IOS surfactant desirable in chemical flooding system. Variable tail length gives IOS surfactant the potential to be used in reservoirs with different salinities (Barnes et al. 2010).

In summary, wettability and interfacial tension are critical factors that dominant recovery efficiency. They are both affected by temperature and composition of displacing phase. When applying chemicals in thermal recovery methods, more understanding is needed on both the effect of chemicals on interface properties and the stability of those additives at high temperature. Unfortunately, studies on the application of chemicals at steam temperature are limited. This study is a continuation of our previous work (Wei and Babadagli 2016) and aimed at screening effective additives to the steam application in carbonates. Novel chemicals (high pH solution, ionic liquid, a cationic surfactant, IOS surfactant, and nanoparticles) were further tested at high temperature and high pressure. At first, the thermal stability of different chemical agents was measured with TGA. Then the effect of chemicals on IFT and wettability at high temperature were evaluated separately. Finally, the comprehensive effect of temperature, chemical additives on production was studied with imbibition tests.

3.3 Materials and Experiments

3.3.1 Oil phase. Crude oil was obtained from the reservoir in eastern Alberta, Canada. The viscosity was measured as 6,000 cp at 25°C. The density of oil at 25°C, atmospheric pressure, and 180°C, 185 psi was 0.997 g/cm³ and 0.899 g/cm³.

3.3.2 Aqueous phase. Aqueous phases were prepared by mixing chemicals in deionized water. **Table 8** summarizes the chemical agents tested in this research. The chemicals were chosen based on the results of our previous screening tests at 90°C (Wei and Babadagli 2016). Tap water was used as the reference to evaluate the performance of other chemicals. Dodecyl trimethylammonium bromide (C12TAB) and 1-Butyl-2, 3-dimethylimidazolium tetrafluoroborate (BMMIM BF₄) were obtained from SIGMA, while LTS-18 was offered by Shell Chemicals. Sodium metaborate solution was prepared with sodium metaborate tetrahydrate (NaBO₂), which was provided by ACROS ORGANICS. Silicon oxide (SiO₂), aluminum oxide (Al₂O₃) and zirconium oxide (ZrO₂) nanofluids were prepared with nanopowder dispersion with sizes 5-35 nm, 10 nm, and 45-55 nm, respectively. Nanopowder dispersions were obtained from US Research Nanomaterials, Inc. The concentrations of solutions were optimized based on IFT, which was demonstrated in the other paper (Wei and Babadagli 2016).

Table 8. List of Chemicals Tested in Chapter 3

Chemical category	Chemical name	Concentration, %wt
Base case	Tap water	
High pH solution	NaBO ₂	1.50
Ionic liquid	BMMIM BF ₄	1.00
Cationic surfactant	C12TAB	0.75
IOS	LTS-18	1.00
Nanofluids	SiO ₂	1.00
	Al ₂ O ₃	0.75
	ZrO ₂	1.00

3.3.4 Substrates and cores. Indiana limestone and Berea sandstone cores with a diameter of 38 mm were used as porous media in the imbibition tests. To establish their original oil-wet state, the Indiana limestone cores were saturated for one week and aged for two weeks at 80°C, while Berea sandstone cores were aged for five weeks. The porosity was calculated from the difference of weight between and after saturation. Detailed information of cores is summarized in **Tables 9** and **10**. In addition to limestone and sandstone plates, contact angles were also measured on calcite and mica substrates as they are good representatives of the minerals in typical carbonate and sandstone samples. Plates and substrates were aged in oil 70°C for one week and then extra oil was removed with toluene carefully.

Table 9. Limestone Imbibition Experiment Data

	Core diam., mm	Core height, mm	PV, cm^3	Porosity, %	Chemical	Conc., %wt
L1	38.4	87.1	9.88	9.79	Tap water	
L2	38.5	87.2	10.21	10.51	$NaBO_2$	1.50
L3	38.2	87.2	11.45	11.45	Ionic liquid	1.00
L4	38.0	87.1	10.48	10.61	C12TAB	0.75
L5	37.1	87.0	10.52	11.19	Al_2O_3	0.75
L6	38.3	82.1	10.62	11.23	ZrO_2	1.00
L7	38.0	82.0	10.48	11.27	LTS-18	1.00

Table 10. Sandstone Imbibition Experiment Data

	Core diam., mm	Core height, mm	PV, cm^3	Porosity, %	Chemical	Conc., %wt
S1	38.3	82.1	17.53	18.53	Tap water	
S2	38.4	82.5	16.91	17.70	$NaBO_2$	1.50
S3	37.9	82.4	16.52	17.77	Ionic liquid	1.00
S4	38.1	82.0	17.09	18.28	Al_2O_3	0.75
S5	38.0	82.1	17.45	18.74	ZrO_2	1.00
S6	38.0	82.5	16.62	17.76	LTS-18	1.00

3.3.5 Thermogravimetric analysis (TGA). TGA is the most widely used technique to evaluate the thermal stability. Cary 670 FTIR Spectrometer was adopted as analyzer in this study. 15 mg of chemical powder was tested under constant nitrogen flow (25 ml/min) and constant heating rate (15°C/min). The samples were heated up to 400°C and the weight loss was recorded versus time.

3.3.6 Contact angle and interfacial tension measurements. Contact angle and IFT (pendant drop method) were measured with the IFT device shown in **Figure 37** at 180°C and 185 psi. Static contact angles of oil on limestone, sandstone plates, calcite and mica substrates were measured in the existence of chemical solutions. Five different chemicals and tap water were used in the measurements. The interfacial properties in LTS-18 and ZrO_2 were not included in this paper because their solutions were opaque and do not meet the optical requirement of the measurement.

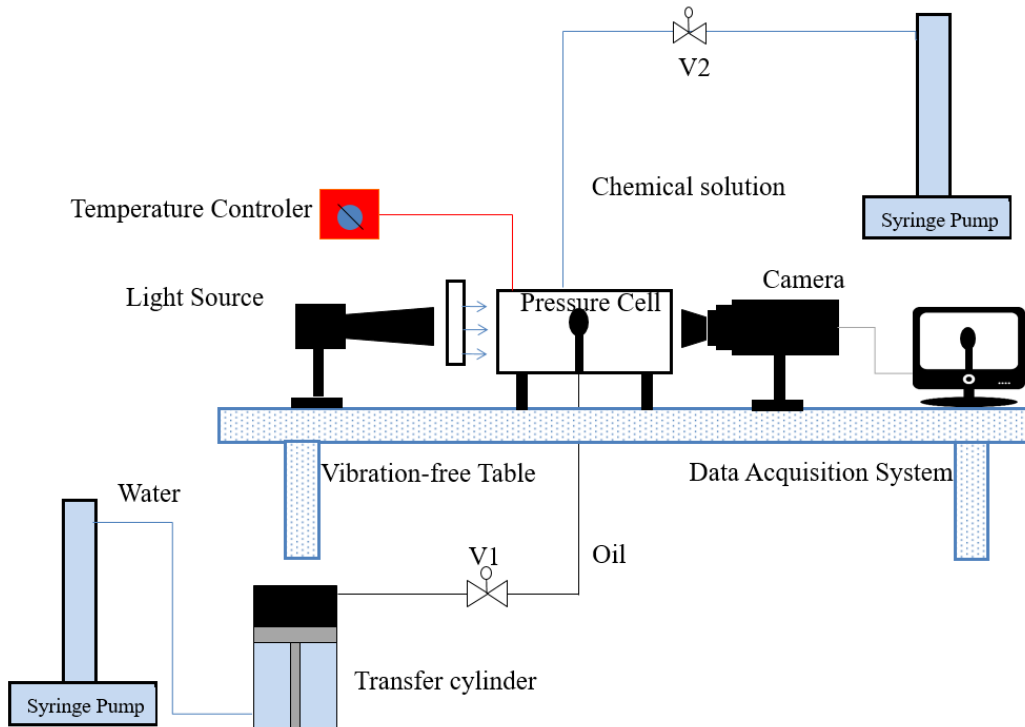


Figure 37. IFT setup used to measure IFT and contact angle.

3.3.7 Capillary imbibition. Imbibition test is an efficient experiment method to investigate the contribution of viscous force, capillary force, and gravity force. However, there are rare documents of the test at a temperature higher than 70°C, let alone as high as 180°C. In this research, imbibition tests were conducted at 90°C and 180°C. The experiment at 90°C was described in detail in our previous paper (Wei and Babadagli 2016). The imbibition tests at 180°C were conducted with specially designed pressure cell (**Figure 38**). The pressure cell was preheated to 100°C to shorten the heating time, which was about 5 hours. The Amott cell contained a saturated core and 80 ml chemical solution was placed in the pressure cell. Then the oven temperature as increased to 180°C and the whole system was pressured up to 185 psi by injecting nitrogen. This pressure value was chosen to make sure the evaporation was less than 1ml in 12 h. The volume of produced oil was observed through the window and was recorded versus time for 12 h.

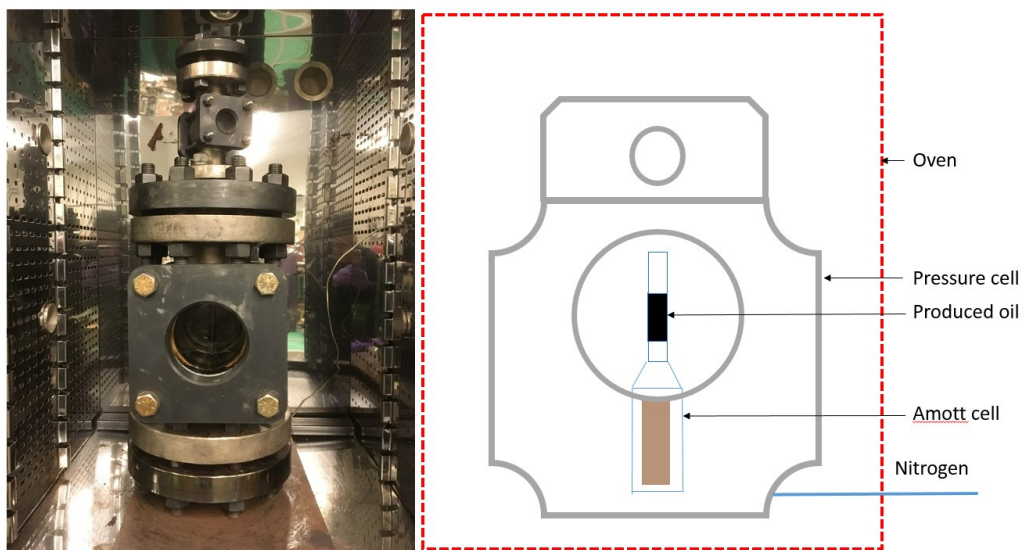


Figure 38. High-temperature high-pressure imbibition setup.

3.4 Results

3.4.1 Thermogravimetric analysis. The thermal stabilities at an elevated temperature of 6 tested chemicals were investigated with TGA. **Figure 39** shows the change of weight of different chemicals as a function of temperature. **Table 11** shows that the weight loss of most chemicals except NaBO_2 were less than 1% at 180°C . In Figure 39, BMMIM BF_4 , SiO_2 , Al_2O_3 and ZrO_2 are thermally stable within measurement temperature range, which was 30 to 400°C . The high weight loss of NaBO_2 is contributed to the dehydration sodium metaborate tetrahydrate, which theoretically contains 52.25% wt. of water. Thus, based on TGA results, all six tested chemicals have the potential to be used at the experiment temperature of this study (180°C). However, it should be noticed that TGA results can only be treated as a reference to screen proper chemicals for thermal application. The stability may be overestimated because TGA only revealed the short-term stability as the temperature increased rapidly during the test (Cao and Mu 2014). Moreover, besides the decomposition of pure chemicals, the stability of chemical solutions is also important, which would be discussed in the imbibition part.

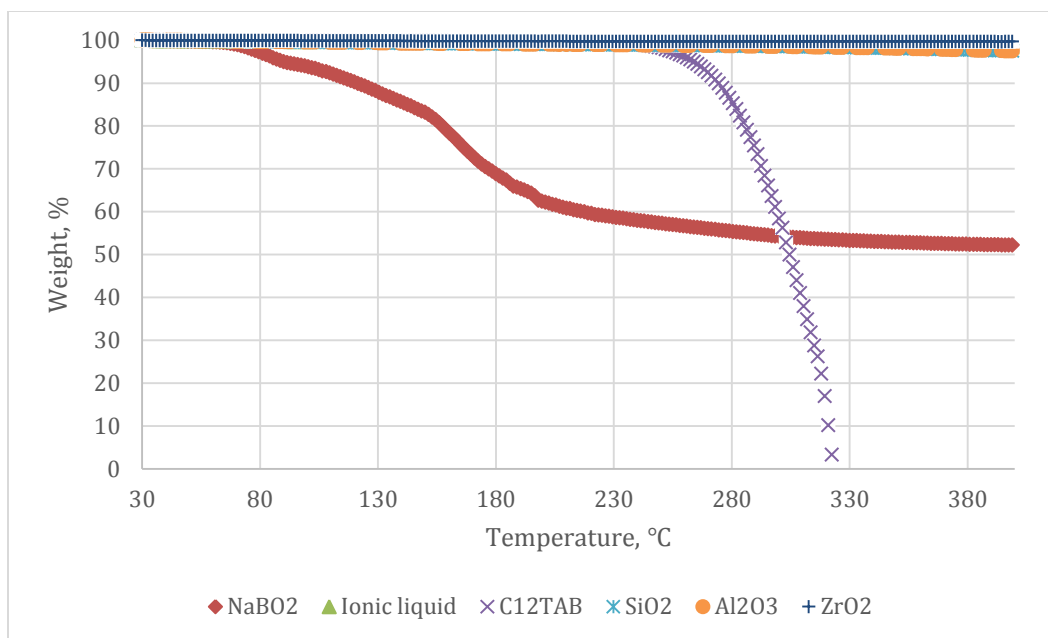


Figure 39. Thermogravimetric analysis of tested chemicals.

Table 11. Weight fraction at 180°C.

Chemical name	Weight, %
$NaBO_2$	60.81
$BMMIM BF_4$	99.39
C12TAB	99.68
SiO_2	99.19
Al_2O_3	99.06
ZrO_2	99.75

3.4.2 Contact angle measurements. The contact angle is the most direct parameter to indicate the wettability of a solid surface. Contact angles in the aqueous phase were measured on different surface at 180°C. A larger contact angle refers to a more water-wet state. **Table 12** shows calcite substrates were strongly oil-wet in tap water at 25°C and the wettability were not improved by increasing temperature. Mica substrates were changed from water-wet to oil-wet as temperature was increased from 25°C to 180°C.

Table 12. Contact Angles of Oil in Tap Water at 25°C, 90°C (Wei and Babadagli 2016), and 180°C

Temperature, °C	Contact angle on calcite, °	Contact angle on mica, °
25	145.70	67.70
90	165.05	127.80
180	161.65	132.85

Figure 40 and **Figure 5** summarize the contact angles measured in different chemical solution at 180°C. The difference between mineral substrates and core plates is owing to the roughness and heterogeneity of core plates. The measurements on Indiana limestone and Berea sandstone are more practical and would be used to analysis the imbibition process, while the results on calcite and mica are more representative of the capability of different chemicals to alter wettability.

Figure 40 shows that contact angle on limestone plates is larger than that on calcite substrate in the same solution. We can also observe that the contact angles on calcite were larger than 90° in all solutions at 180°C. Among four tested chemicals, BMMIM BF₄ and NaBO₂ had the ability to change calcite surface to be more water-wet. The contact angle in BMMIM BF₄ solution was about 40° smaller than that in tap water. Al₂O₃ nanofluid had little influence on the wettability at that temperature, while the calcite was completely oil-wet in C12TAB solution. As seen in **Figure 41**, mica surface is more oil-wet than Berea sandstone in the same chemical solution except Al₂O₃ nanofluids. BMMIM BF₄, SiO₂, Al₂O₃ changed the mica from oil-wet to water-wet at 180°C and NaBO₂ reduce contact angle on mica by 40°. However, in C12TAB solution, mica was completely oil-wet, which is consistent with the observation on calcite.

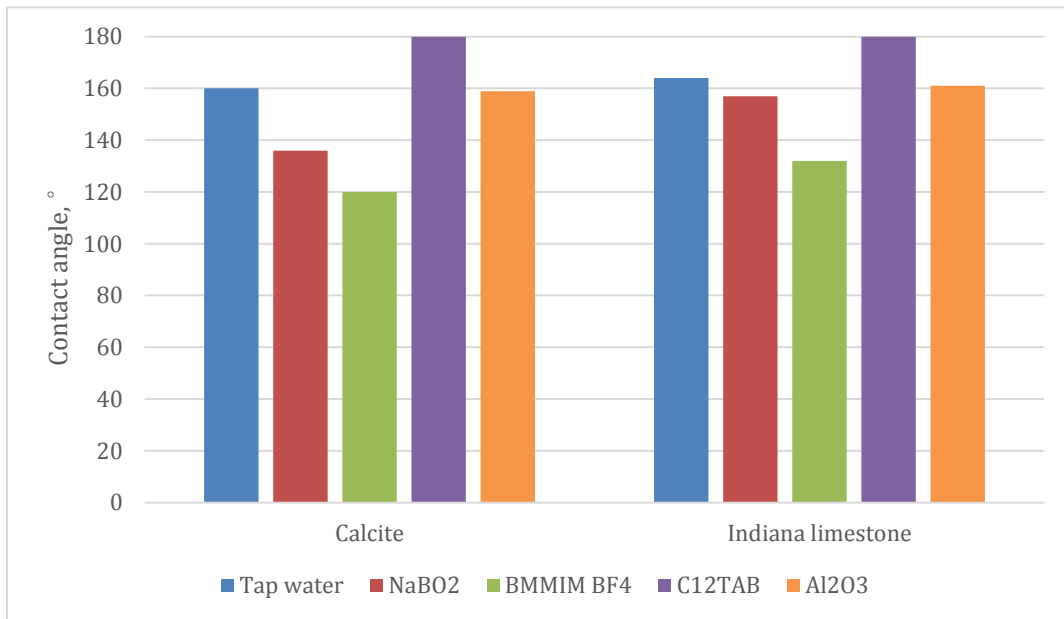


Figure 40. Contact angle on calcite and Indiana limestone measured at 180°C.

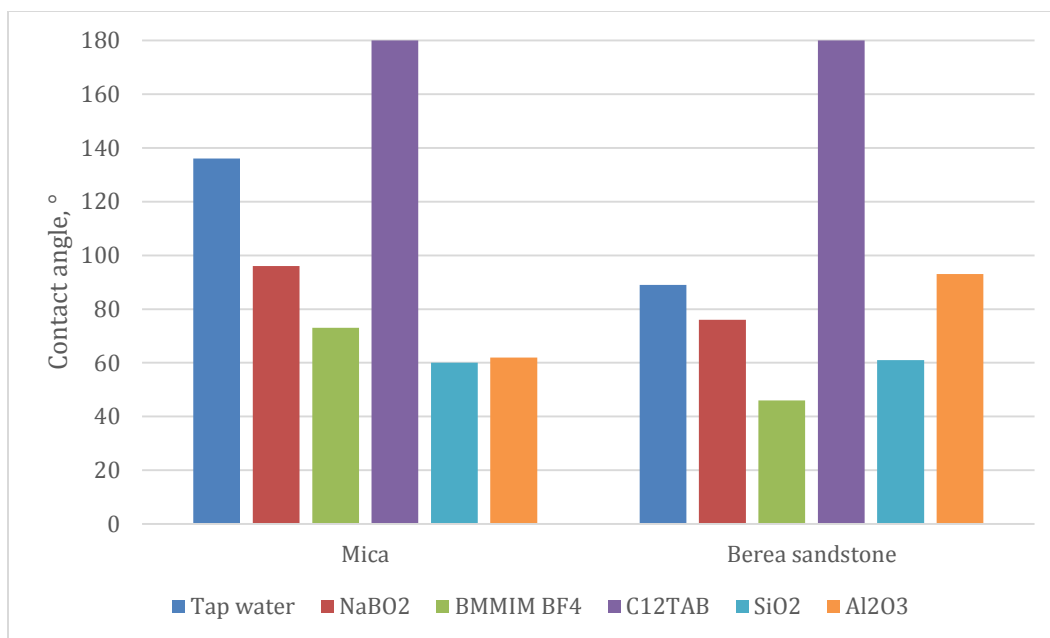


Figure 41. Contact angle on calcite and Indiana limestone measured at 180°C.

The comparison of contact angle at different temperatures demonstrates the thermal resistance of different chemicals. As presented in **Figure 42**, all chemicals can increase the water-wettability of calcite at 25°C. The capability of BMMIM BF₄ and NaBO₂ was not impaired by increased temperature because of their good thermal stability. However, the contact angle in C12TAB solution increased from 46.5° to 180° as the temperature increased from 25 °C to 180°C. **Figure 43** shows the spreading process of an oil droplet on calcite when the temperature was increased. C12TAB, as a cationic surfactant, is claimed to change the wettability by first forming ion-pairs between negatively charged carboxylate components adsorbed on the surface and the cationic head. Then ion-pair is further stabilized by hydrophobic interaction (Standnes and Austad 2003). High temperature can cause both the decomposition of C12TAB and the break of weak hydrophobic interaction. The duration of the experiment is short to see the thermal instability effect of C12TAB.

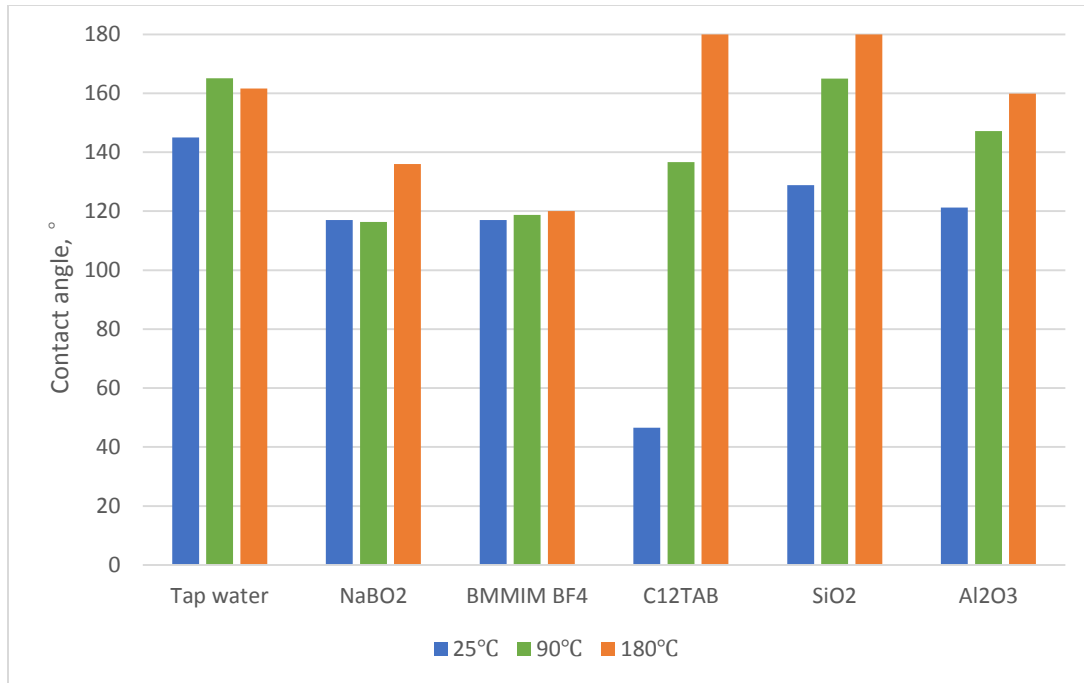


Figure 42. Comparison of contact angles at 25°C, 90°C (from Wei and Babadagli 2016), and 180°C.



Figure 43. Oil droplets on calcite surface in C12TAB solution at 60°C, 90°C, and 120°C.

The contact angle in SiO₂ and Al₂O₃ nanofluids also gradually increased with increasing temperature. The mechanism of wettability alteration induced by nanoparticles is suggested to be related to the adsorption of nanoparticles on oil/brine/surface contact region (Wasan and Nikolov 2003; Karimi et al. 2012). However, this adsorption is thermally unstable and can be easily removed at high temperature. The imbibition tests will reveal more (and complementary) information on the wettability alteration and thermal stability of the chemicals as its duration is longer than IFT and contact angle experiments.

3.4.3 Interfacial tension measurements. The interfacial tension of oil and tap water at 25°C and ambient pressure was documented as 28.35 mN/m, which suggested that the tested crude oil was free of surface active components. In this work, IFT between oil and solutions were measured at

180°C and 185 psi to investigate the comprehensive result of pressure, temperature and chemical agents. The IFT values are shown in **Figure 44**. Compared with the IFT in tap water (2.00 mN/m), NaBO₂, C12TAB, SiO₂ and Al₂O₃ nanoparticles reduced the interfacial tension, while BMMIM BF₄ led to a higher IFT.

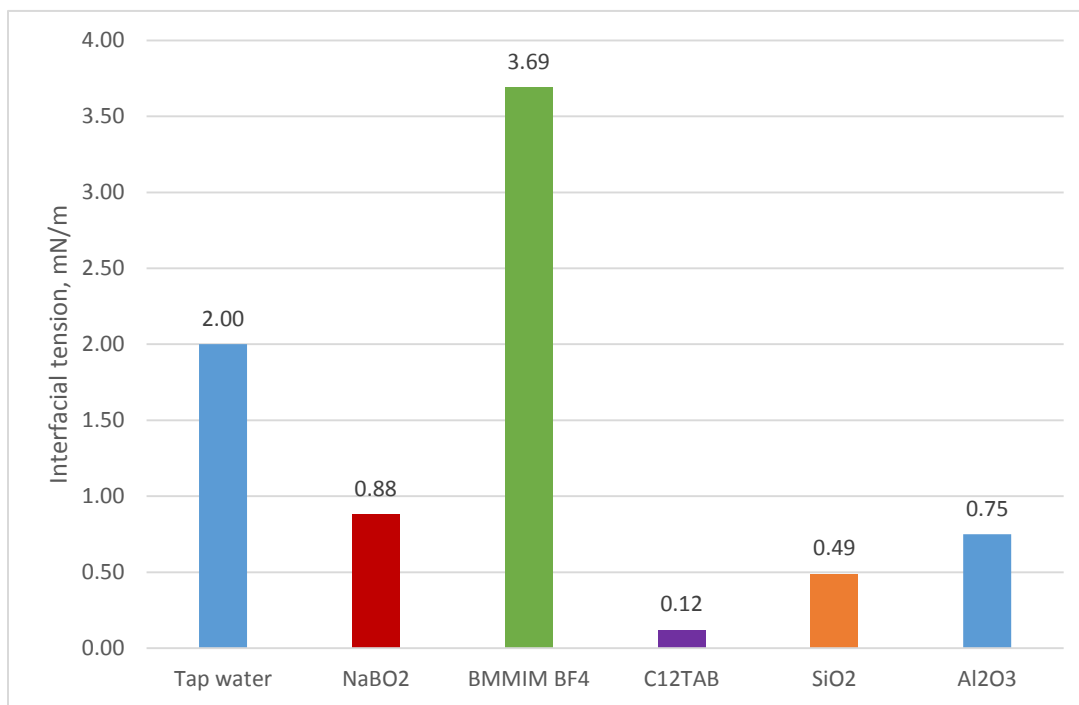


Figure 44. IFT between oil and different chemical solution at 180°C and 185 psi.

As can be inferred from **Figure 45**, with NaBO₂ dissolved in water, the interfacial tension decreased from 2mN/m to 0.88 mN/m. The reduction of IFT of oil in alkalis solution can be attributed to the formation of in situ soap between alkalis and the acidic component in the crude oil (Jeff and Wasan 1993). Considering the low IFT at 180°C, NaBO₂ maintain its capability of reducing IFT between oil and water at high temperature.

The interface between crude oil and BMMIM BF₄ solution had the highest interface energy. As shown in Figure 45, IFT measured at 60°C and 90°C in this ionic liquid solution was higher than that in tap water at the same temperature. This phenomenon cannot be explained by existing data but may be related to the solvent nature of BMMIM BF₄ rather than having surfactant characteristics.

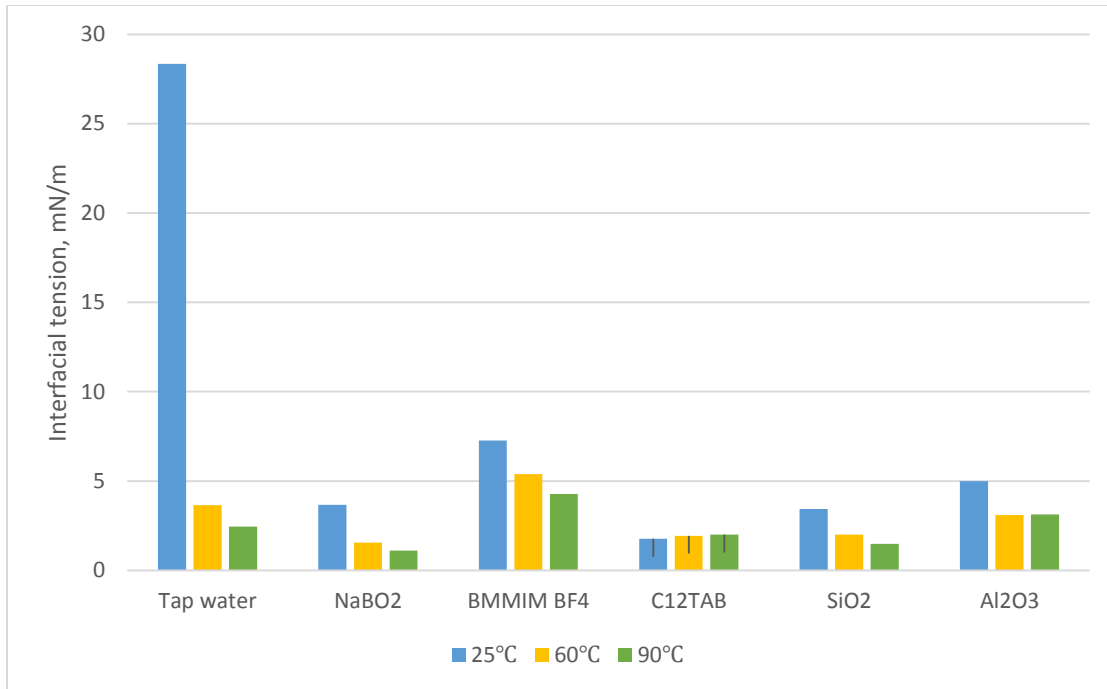


Figure 45. Comparison of IFT at 25°C, 60°C and 90°C, 14.7 psi (from Wei and Babadagli 2016).

At 180°C and 185 psi, the minimum IFT was observed in C12TAB, which was only 0.12 mN/m. However, Figure 45 shows the influence of temperature on the IFT between oil and C12TAB solution. The IFT of C12TAB was measured at a surface aged for 300s rather than equilibrium. Hence, the bars indicate that the actual values were lower than the values in this figure. From Figure 45, one may observe that there is an increasing trend of interfacial tension as temperature increased from 25°C to 90°C.

The interfacial tension in SiO₂ nanofluid was lower than in Al₂O₃ nanofluid. Nanoparticles are reported to be able to modify the interfacial tension in oil/water system by previous experimental and simulation works (Fan and Striolo 2012; Khehrnejad et al. 2015; Roustaei et al. 2012).

3.4.4 Capillary imbibition. Capillary imbibition test is one of the most widely used experiment tools to evaluate the wettability condition of core samples. Besides wettability condition, the production curve obtained in imbibition test also gives an idea about interfacial tension change and the contribution of gravity force and capillary force. Although imbibition tests have been extensively adopted for decades, the application of imbibition was limited to low temperature and atmospheric pressure because of the evaporation of water and poor bearing pressure ability of the Amott cells. In this work, imbibition test was conducted at 180°C and 185 psi with special

pressure cell. The results from imbibition test were combined with contact angle and IFT data to have a better understanding of the comprehensive effect of pressure, temperature and the application of different chemical agents.

3.4.4.1 Effect of pressure. To be in the liquid phase for water to ensure capillary imbibition transfer, the pressure was increased using nitrogen according to the temperature applied, which was 180°C. From **Figure 46**, one may observe after being soaked in water for 12 h, only 7.74% oil was expelled from the core because of the strong oil-wetness of Indiana limestone. Since the theoretical amount of expelled oil by thermal expansion was calculated as 8.17%, we can state that the production at 180°C and 185 psi was totally due to this mechanism. By decreasing pressure by 25 psi, 500% more oil was recovered from the limestone core in 10 h. This dramatic increase is caused by many reasons: (a) Buoyancy force of gas bubble assisted the rise of oil; (b) density difference between water and oil increased at a lower pressure, and; (c) IFT change between oil and water decreased with decreasing pressure. Thus, 185 psi was adopted for the following imbibition tests to avoid the influence of buoyancy force and to control the evaporation within an acceptable level (1 ml per 12 h).

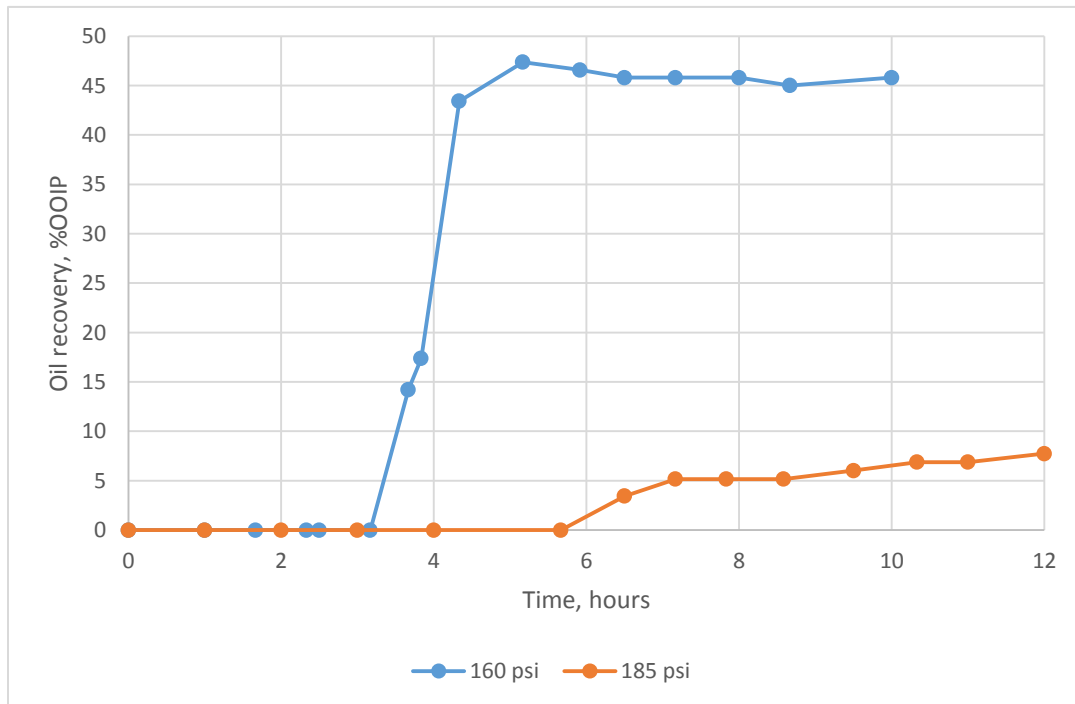


Figure 46. Oil recovery vs. time from limestone cores in tap water at 180°C.

3.4.4.2 Effect of different chemical agents on Indiana limestone. The recovery curves from Indiana limestone cores in different solutions at 180°C and 185 psi are presented in **Figure 47**. In general, compared with the base case with tap water, BMMIM BF₄, ZrO₂ nanoparticle and LTS-18 improve the production, NaBO₂ and C12TAB had little influence on final recovery factor, while Al₂O₃ nanoparticles impaired the production process. In the following part the flow mechanism, production rate, and final recovery would be analyzed based on the interface properties (**Figure 48**) and thermal stabilities mentioned in the previous section.

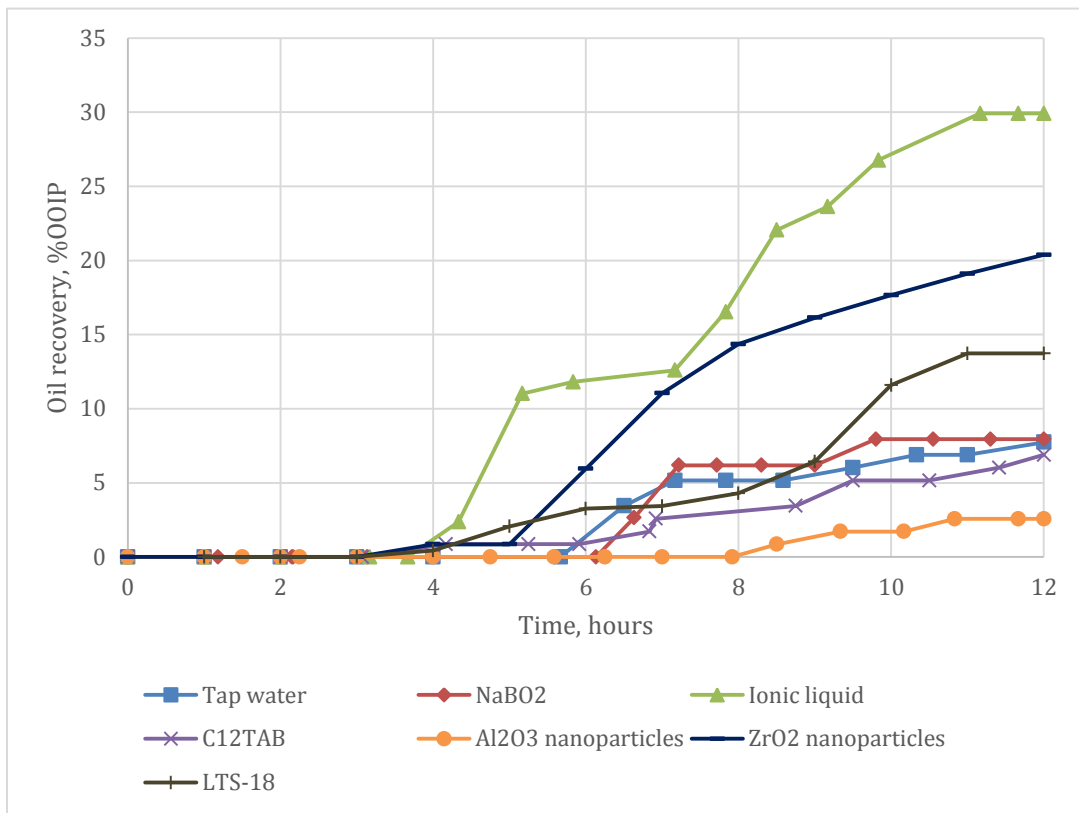


Figure 47. Oil recovery vs. time in limestone cores at 180°C and 185 psi.

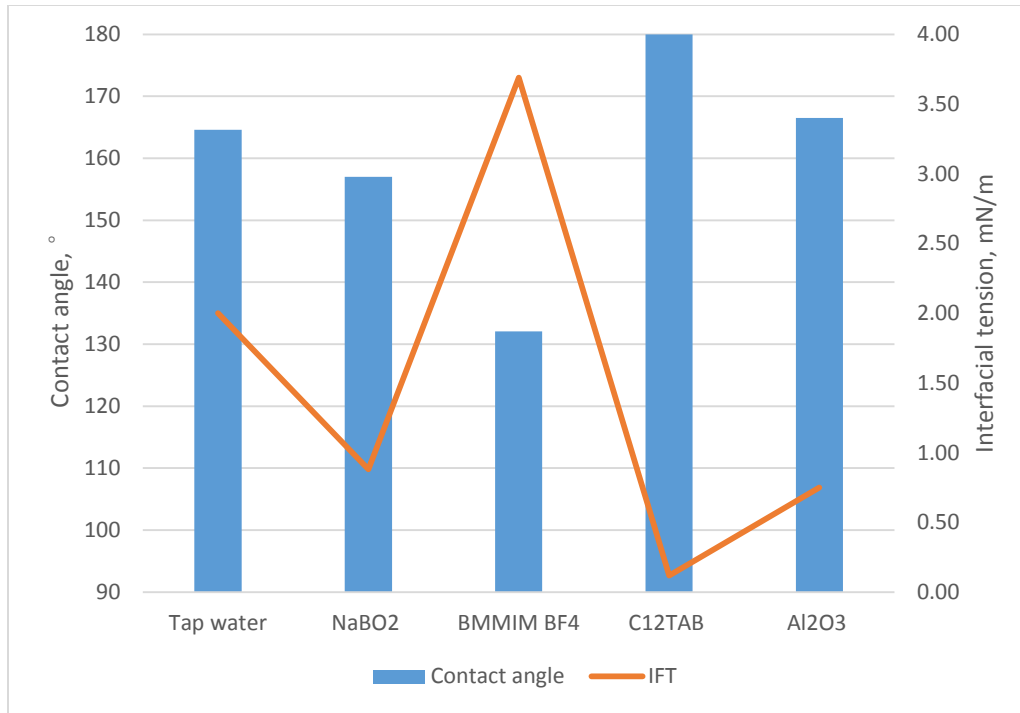


Figure 48. Summary of surface properties in oil/ limestone solutions at 180°C and 185 psi.

Among all the tests, the limestone core in BMMIM BF₄ solution produced most oil, 30% OOIP in 12 hours. As shown in Figure 47, most oil was produced in two stages. Stage 1 occurred between 4.33 to 5.16 h, when the temperature was lower than 180°C. The IFT information was unknown, but as proved in our previous work, the capability of BMMIM BF₄ to improve wettability was relatively stable at the temperature range 90 to 200°C (Wei and Babadagli 2016). The high production rate can be attributed to the improvement of wettability and thermal expansion. In the second stage (7.16 to 11.16 h), system temperature and pressure were stabilized at 180°C and 185 psi. Figure 48 shows that the contact angle was smallest in BMMIM BF₄ solution, which indicated a most water-wet state. The resistance force caused by unfavorable reduced and oil was produced with assistance by gravity force.

In Figure 47, the recovery curve in NaBO₂ solution was similar to the curve in tap water. The cores in both solutions started to produce oil around 6 h and ended in about 8% OOIP production. The curves indicate that the production in NaBO₂ solution shared the same mechanism with that in tap water, which was the combination of thermal expansion and gravity force. Hence, although NaBO₂ reduced both contact angle and IFT, its effect was not big enough to change the flow pattern.

The most important characteristics of the C12TAB curve were the early starting time and relatively low recovery factor in 12 h. The production in C12TAB solution started earliest among all test, which was 4.16 h. At that time, the temperature was lower than 180°C and the rock was not completely oil-wet. Also, the IFT change was very low. During this period, gravity might be the dominant mechanism. After 12 h, however, only 6.88% oil was recorded, but the plateau was not reached at that time. Higher ultimate recovery factor was expected for a longer time because of the very low IFT value between oil and C12TAB solution, which controls the final distribution and trap of oil in pores.

For the core in Al₂O₃ Nanofluid, the production was delayed and the recovery by 12 h was as low as 2.57% OOIP. The behavior was contradicted to the measured surface properties and may be related to instability of nanofluids at high temperature.

LTS-18 and ZrO₂ nanofluid was not tested in the contact angle and IFT part in this study because of the cloudy nature of the solution. However, the imbibition test proved that they had the capability of enhancing oil production from limestone. In ZrO₂ nanofluid, more than 20% oil was expelled after 12 h, which was also documented in the literature (Cao et al. 2016; Mohammed and Babadagli 2014; Wei and Babadagli 2016). LTS-18 also had good performance in the test in limestone. The recovery factor in it was improved by 163.3% compared with in tap water. More work is needed in the future to properties and applications of LTS-18 and ZrO₂ nanoparticle in EOR.

Figure 47 indicates that the ionic liquid and ZrO₂ showed a similar trend of imbibition and quicker recovery in the early stages. This indicates that their role is wettability alteration also corroborated by the contact angle values obtained for the former in Figure 48 and for the latter as reported by Mohammed and Babadagli (2014) and Cao et al. (2016). Other chemicals contributed to the recovery by IFT change at higher temperatures, which eventually accelerated the gravity drainage.

3.4.4.3 Effect of different chemical agents on Berea Sandstone. The production curves in Berea sandstone cores in different chemical solutions are shown in **Figure 49**. All five chemicals used in this test led to a higher recovery factor than tap water. The highest recovery was from the core in NaBO₂ solution. After 12 hours, the core in NaBO₂ solution produced 22.93% OOIP. The

cores in BMMIM BF₄ and LTS-18 gave similar production (23% OOIP) by the end of the test. Crude oil produced in Al₂O₃ nanofluid was 15.83% OOIP, which was 10.54% more than the recovery in SiO₂ nanofluid.

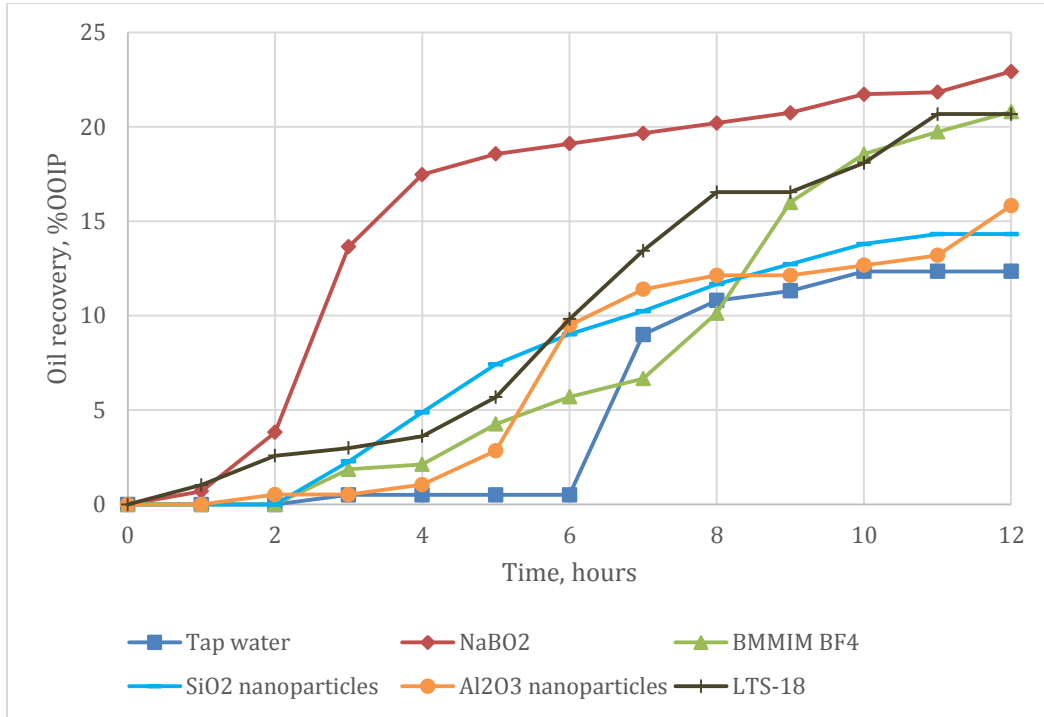


Figure 49. Oil recovery vs. time in sandstone cores at 180°C and 185 psi.

It can be inferred from Figure 49 that the production curve in Al₂O₃ is similar to the curve in tap water in the first 11 hours. In those two solutions, a slight amount of oil was produced in the heating stage (the first 5 hours). Then oil was expelled out of cores rapidly (6.97% OOIP in the 6th hour in Al₂O₃ and 8.49% OOIP in the 7th hour in tap water). The rapid production stage was followed by the slow increase in the next 5 hours. According to the interfacial properties summarized in **Figure 50**, Berea sandstone is neutral-wet in tap water and Al₂O₃ nanofluid. Therefore, the similarity in curves is owing to the similar driving force, which was dominant by gravity force rather than capillary force. However, although tap water and Al₂O₃ led to similar wettability, the interfacial tension in Al₂O₃ was as low as 0.75, which was only 37.5% of the interfacial tension in tap water. As mentioned in the previous section, low interfacial tension leads to high final recovery. Hence, the recovery factor in Al₂O₃ was higher than in tap water and the production did not reach a plateau by the end of 12 hours in Al₂O₃ nanofluid.

The production in both BMMIM BF₄ solution and SiO₂ nanofluid started after 2 hours. For the core in BMMIM BF₄ solution, the recovery did not reach the maximum in the test and production rate was high at 180°C and 185 psi (in the last 7 hours). As shown in **Figure 50**, the system had the highest interfacial tension and smallest contact angle in BMMIM BF₄ solution. Therefore, BMMIM BF₄ solution gave the system biggest capillary force, which worked with gravity force and contributed to the continuous high production rate. The similarity in the curves for LTS-18 and BMMIM BF₄ indicates that they share similar flow pattern. The production in the sandstone core with SiO₂ started at the same time as in BMMIMBF₄, but the rate gradually decreased and ended in 30.69% less recovery in 12 hours. According to the contact angle results in Figure 50, the sandstone in SiO₂ is less water-wet than in BMMIM BF₄. Therefore, both average production rate and recovery factor in SiO₂ are lower than in BMMIM BF₄ solution. However, considering the low interfacial tension in SiO₂ nanofluid, more oil was expected in a longer period.

Among the 6 tests in this research, the core in NaBO₂ solution had the biggest recovery factor in 12 hours. However, 80.94% of the expelled oil was recorded in the first five hours. The high recovery rate in the heating stage is related to the favorable interfacial properties in NaBO₂ at low temperature (Wei and Babadagli 2016). After the system was heated to 180°C, oil was expelled at a slow and constant speed and did not get the equilibrium because of the low interfacial tension.

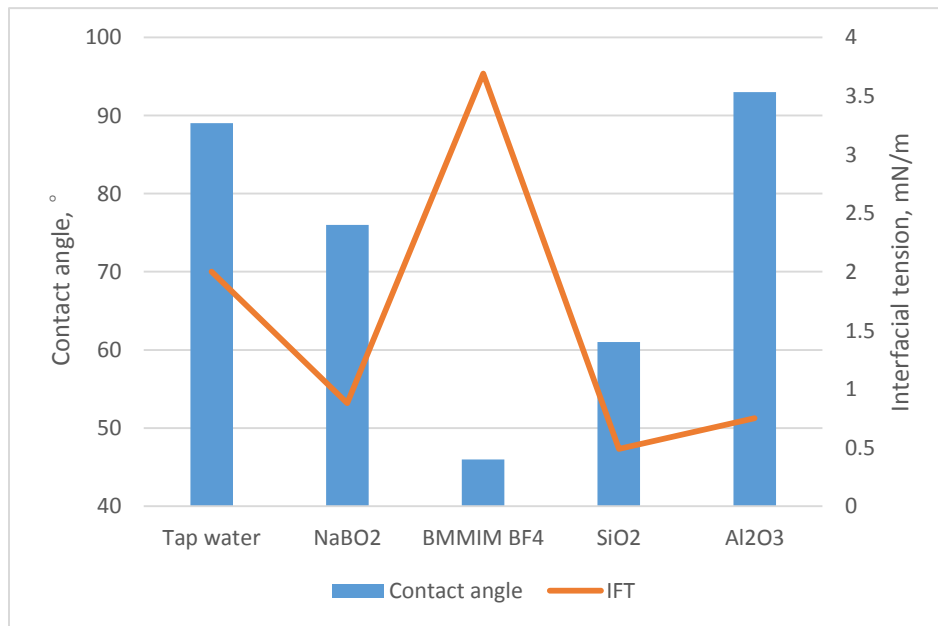


Figure 50. Summary of surface properties in oil/ sandstone solutions at 180°C and 185 psi.

3.5 Conclusions

A group of new chemicals was tested as a steam additive for recovery improvement of heavy-oil for limestone and sandstone at steam temperature. Their thermal stability was measured using TGA up to 400°C. The capability of different kinds of chemical agents on modifying surface properties was evaluated by contact angle and interfacial tension measurement. Imbibition test was conducted at high temperature and high pressure for the first time. The comprehensive effect of pressure, temperature, and chemical additives was studied with imbibition tests.

Ionic liquid BMMIM BF₄ had the ability to decrease contact angle in both limestone and sandstone. Although the IFT in BMMIM BF₄ was higher than the IFT in tap water, the production in the core test was increased, which was attributed to its wettability alteration capability. Considering its environmentally friendly nature, BMMIM BF₄ is a promising chemical as a steam additive.

NaBO₂ is thermally stable and can reduce the interfacial tension at high temperature and high-pressure condition. However, it showed the relatively small effect on the recovery factor in the limestone because it has limited capability for wettability alteration at higher temperatures. The influence in heavy oil sandstone system at steam temperature is not clear since most of the oil came out in the heating stage.

C12TAB can reduce both contact angle and IFT at low temperature. However, it is thermally unstable at elevated temperatures. Both limestone and sandstone in C12TAB solution were completely oil-wet at 180°C. Hence, it may not be a good choice for the thermal applications.

Al₂O₃ nanoparticle cannot increase thermal recovery in limestone, while had good performance in sandstone. The production in sandstone was enhanced by Al₂O₃, as it improved both the wettability and interfacial tension in heavy oil/sandstone system. SiO₂ is another good candidate for the thermal application in sandstone because of the capability of improving wettability. But, since nanoparticles settle down in water at high temperature, more work is needed on improving the stability of nanofluids.

LTS-18 and ZrO₂ nanoparticles have the potential to be used at steam temperature, but the mechanism of enhancing oil recovery needs to be identified through further research.

Chapter 4: Conclusion and Future Work

4.1 Conclusions and Contributions

A group of novel chemicals was studied as interfacial modifiers for sandstone and limestone at elevated temperature and pressure. Their thermal stability was tested with TGA up to 400°C. Their effect on wettability and interfacial tension were evaluated at different temperature and pressure condition. The mechanism of wettability alteration was further investigated with AFM tests. Imbibition tests were carried out at steam temperature for the first time in a newly-designed pressure cell to study the comprehensive of chemicals, pressure, and temperature on production.

$NaBO_2$ exhibited good thermal stability in interfacial modification. It helped to improve recovery in the limestone at 90°C but it is not recommended to be used at steam temperature.

Ionic liquid BMMIM BF_4 was capable of improving wettability in both sandstone and limestone because it can remove the adsorbed oil on the surface. It had the best performance among all tested chemicals in heavy-oil/limestone system. Considering the thermal stability and environmental friendliness, BMMIM BF_4 is a promising chemical additive.

C12TAB was efficient in reducing contact angle and wettability at low temperature. However, it is unstable at high temperature, thus impairing thermal recovery process.

SiO_2 nanoparticle was more efficient in reducing interfacial tension than Al_2O_3 nanoparticle at both 90°C and 180°C. It is a good candidate as the chemical additives in the thermal application.

IOS LTS-18 and ZrO_2 nanoparticle were observed to increased the recovery from both sandstone and limestone at elevated temperature. However, their effect on interfacial properties of heavy-oil/water/rock system is not clear yet.

4.2 Limitations and Future Work

Aside from pressure and temperature, the phase of displacing fluid is another factor that affects the wettability of reservoir work. The evaluation of steam-induced wettability alteration in different rock/bitumen/steam system and the analysis of the mechanism of wettability change caused by the change of the phase of water and chemical additives are needed.

LTS-18 and ZrO_2 nanoparticles have the potential to be used at elevated temperature. However, their effect on the wettability and interfacial tension was not included in this thesis because of the limitation of the IFT device and visualization problems. Evaluation of interfacial properties in LTS-18 and ZrO_2 nanoparticles with other methods is suggested to gain a better understanding of their working mechanism.

The thermal stability of SiO_2 , Al_2O_3 and ZrO_2 nanoparticle was tested in this research but the stability of the solutions was ignored. Nanoparticles settled down in water at high temperature. More efforts are needed on improving the stability of nanofluids.

References

Chapter 1:

- Buckley, S. E., & Leverett, M. C. 1942. Mechanism of Fluid Displacement in Sands. *Society of Petroleum Engineers*. doi: 10.2118/942107-G.
- Cao, N., Mohammed, M. and Babadagli, T. 2016. Wettability Alteration of Heavy-Oil/Bitumen Containing Carbonates Using Solvents, high pH Solutions and Nano/Ionic Liquids. *SPE Res. Eval. and Eng.* **20**: 363-371. doi:10.2118/183646-PA.
- Chen, P., & Mohanty, K. K. 2014. Wettability Alteration in High Temperature Carbonate Reservoirs. *Society of Petroleum Engineers*. doi:10.2118/169125-MS.
- Frauenfeld, T., Jossy, C., and Wang, X. 2007. Experimental studies of thermal solvent oil recovery process for live heavy oil. *J. Can. Pet. Technol.* **46**: 40–46. doi:10.2118/07-11-03.
- Green, K. and Malcolm, J. D. 1985. Laboratory Studies Of Surfactant Additives To Steam For The Recovery Of Bitumen From Oil Sand. Annual Technical Meeting, Edmonton, Alberta, June 2 – 5. PETSOC-85-36-25. doi:10.2118/85-36-25.
- Handy, L. L., Amaefule, J. O., Ziegler, V. M., et al. 1982. Thermal Stability of Surfactants for Reservoir Application (includes associated papers 11323 and 11597). *Society of Petroleum Engineers Journal* **22** (05): 722-909. SPE-7867-PA. doi:10.2118/7867-PA.
- Hayes, M., Bourrel, M., El-Emary, M., et al. 1979. Interfacial Tension and Behavior of Nonionic Surfactants. *SPE J.* **19**: 349–356. doi:10.2118/7581-PA.
- Mohammed, M. and Babadagli, T. 2015. Wettability Alteration: A Comprehensive Review of Materials/Methods and Testing the Selected Ones on Heavy-Oil Containing Oil-Wet Systems. *Adv. Colloid Interface Sci.* **220**: 54–77. doi:10.1016/j.cis.2015.02.006.
- Maini, B. B. and Ma, V. 1985. Thermal Stability of Surfactants for Steamflood Applications. SPE Oilfield and Geothermal Chemistry Symposium, Phoenix, Arizona, 9-11 March. doi:10.2118/13572-MS.
- Sharma, J. and Gates, I.D. 2013. Interfacial Stability of In-Situ Bitumen Thermal Solvent Recovery Processes. *SPE J.* **16**: 55–64. doi:10.2118/130050-PA.
- Wagner, O.R. and Leach, R.O. 1966. Effect of Interfacial Tension on Displacement Efficiency. *SPE J.* **6**. doi:10.2118/1564-PA.
- Wang, Y., Xu, H., Yu, W., et al. 2011. Surfactant induced reservoir wettability alteration: Recent theoretical and experimental advances in enhanced oil recovery. *Pet. Sci.* **8**: 463–476. doi:10.1007/s12182-011-0164-7.

Chapter 2:

- Ayatollahi, S. and Zerafat, M. 2012. Nanotechnol. Conf. Noordwijk, the Netherlands, 12–14 June. SPE 157094. <http://dx.doi.org/10.2118/157094-MS>.
- Cao, N., Mohammed, M.A. and Babadagli, T. 2015. Offshore Technology Conference, Rio de Janeiro, Brazil, 27–29 October, OTC-26068-MS. <http://dx.doi.org/10.4043/26068-MS>.
- Chen, P. and Mohanty, K.K. 2014. SPE/DOE Symp. Improv. Oil Recover. Tulsa, Oklahoma, USA, 12–16 April. SPE-169125-MS. <http://dx.doi.org/10.2118/169125-MS>.
- Edmunds, N., Barrett, K., Solanki, S. et al. 2009. *J. Can. Pet. Technol.* **48**: 26–32. PETSOC-09-09-26. <http://dx.doi.org/10.2118/09-09-26>.
- Hamouda, A.A. and Gomari, K.A.R. 2006. SPE/DOE Symp. Improv. Oil Recover. 22-26 April. SPE 99848 1–12. doi:10.2118/99848-MS. <http://dx.doi.org/10.2118/99848-MS>.
- Hogshead, C.G., Manias, E., Williams, P. et al. 2011. *Energy & Fuels* **2011** (25): 293–299. 10.1021/ef101404k. doi:10.1021/ef101404k.
- Jiang, Q., Yuan, J., Russel-Houston, J. et al. 2010. *J. Can. Pet. Technol.* **49**: 56–64. PETSOC-09-09-26. <http://dx.doi.org/10.2118/2009-067>.
- Karimi, A., Fakhroueian, Z., Bahramian, A. et al. 2012. *Energy and Fuels* **26**: 1028–1036.
- Li, S., Genys, M., Wang, K. et al. 2015. SPE Reservoir Characterisation and Simulation Conference and Exhibition, Abu Dhabi, UAE, 14–16 September. doi:10.2118/175610-MS.
- Maghzi, A., Mohebbi, A., Kharrat, R. et al. 2011. *Transp. Porous Media.* **87**: 653–664. doi:10.1007/s11242-010-9696-3.
- Mohammed, M. and Babadagli, T. 2014. SPE Heavy Oil Conf. Calgary, Alberta, Canada, 10–12 June 1–14. SPE-170034-MS. <http://dx.doi.org/10.2118/170034-MS>.
- Mohammed, M. and Babadagli, T. 2015a. *Adv. Colloid Interface Sci.* **220**: 54–77. doi:10.1016/j.cis.2015.02.006.
- Mohammed, M. and Babadagli, T. 2015b. Offshore Technology Conference, Rio de Janeiro, Brazil, 27–29 October. OTC-26068-MS. <http://dx.doi.org/10.4043/26068-MS>.
- Naderi, K., Babadagli, T. and Coskuner, G. 2013. *Energy Fuels* **27**: 6501–6517. 10.1021/ef401333u. <http://pubs.acs.org/doi/abs/10.1021/ef401333u>.
- Ragab, A.M. and Hannora, A.E. 2015. SPE Kuwait Oil and Gas Show and Conf., Mishref, Kuwait, 11–14 October. doi:10.2118/175395-MS.
- Roustaei, A. and Bagherzadeh, H. 2015. *Petrol. Explor. Prod. Technol.* **5**: 27–33. doi:10.1007/s13202-014-0120-3.
- Schembre, J.M., Tang, G.Q., and Kovalscek, A.R. 2016. *J. Pet. Sci. Eng.* **52**: 131–148. doi:10.1016/j.petrol.2006.03.017.

- Torsater, O., Engeset, B., Hendraningrat, L. et al. 2012. SPE Kuwait International Petroleum Conf. and Exhibition, Kuwait City, Kuwait, 10-12 December. doi:10.2118/163335-MS.
- Wasan, D.T. and Nikolov, A.D. 2003. *Nature* **423**: 156–159. doi:10.1038/nature01591.
- Wasserscheid, P. and Keim, W. Chem. 2000. *Int. Ed. Engl.* **39**: 3772–3789. doi:10.1002/1521-3773(20001103)39:21<3772::AID-ANIE3772>3.0.CO;2-5.
- Ye, Z., Zhang, F., Han, L. et al. 2008. *Colloids Surfaces A Physicochem. Eng. Asp.* **322**: 138–141.

Chapter 3:

- Al-Hadhrami, H.S. and Blunt, M.J. 2000. Thermally Induced Wettability Alteration to Improve Oil Recovery in Fractured Reservoirs. SPE/DOE Improved Oil Recovery Symposium, Tulsa, Oklahoma, 3-5 April. doi:10.2118/59289-MS.
- Babu, D. R. A. M., Hornof, V., and Neale, G. 1984. Effects of Temperature and Time on Interfacial Tension Behavior Between Heavy Oils and Alkaline Solutions. *The Canadian Journal of Chemical Engineering* **62** (1): 156-159. doi:10.1002/cjce.5450620124.
- Barnes, J. R., Dirkwager, H., Smit, J. et al. 2010. Application of Internal Olefin Sulfonates and Other Surfactants to EOR . Part 1 : Structure - Performance Relationships for Selection at Different Reservoir Conditions. SPE Improved Oil Recovery Symposium, Tulsa, Oklahoma, USA, 24-28 April. SPE 129766. doi:10.2118/129766-MS.
- Benzagouta, M.S., Al-Nashef, I.M., Karnanda, et al. 2013. Ionic liquids as novel surfactants for potential use in enhanced oil recovery. *Korean J. Chem. Eng.* **30**: 2108–2117. doi:10.1007/s11814-013-0137-1.
- Cao, N., Mohammed, M. and Babadagli, T. 2016. Wettability Alteration of Heavy-Oil/Bitumen Containing Carbonates Using Solvents, high pH Solutions and Nano/Ionic Liquids. *SPE Res. Eval. and Eng.* **20**: 363-371. doi:10.2118/183646-PA.
- Cao, Y. and Mu, T. 2014. A comprehensive investigation on the thermal stability of 66 ionic liquids by thermogravimetric analysis. *Ind. Eng. Chem. Res.* **53**. doi:10.1021/ie5009597.
- Emad Al, M.S. 2013. Experimental Study of Use of Ionic Liquids in Enhanced Oil Recovery. *J. Pet. Environ. Biotechnol.* **4**: 4–10. doi:10.4172/2157-7463.1000165.
- Falls, A. H., Thigpen, D. R., Nelson, R. C., et al. 1994. Field Test of Cosurfactant-Enhanced Alkaline Flooding. *SPE Res. Eng.* **9**: 217-223. doi:10.2118/24117-PA.
- Fan, H. and Striolo, A. 2012. Nanoparticle effects on the water-oil interfacial tension. *Phys. Rev. E - Stat. Nonlinear, Soft Matter Phys.* **86**: 1–11. doi:10.1103/PhysRevE.86.051610.
- Frauenfeld, T., Jossy, C., and Wang, X. 2007. Experimental studies of thermal solvent oil recovery process for live heavy oil. *J. Can. Pet. Technol.* **46**: 40–46. doi:10.2118/07-11-03.

- Green, K. and Malcolm, J. D. 1985. Laboratory Studies of Surfactant Additives to Steam for the Recovery of Bitumen from Oil Sand. Annual Technical Meeting, Edmonton, Alberta, June 2–5. PETSOC-85-36-25. doi:10.2118/85-36-25.
- Hamouda, A. A. and Rezaei Gomari, K. A. 2006. Influence of Temperature on Wettability Alteration of Carbonate Reservoirs. SPE/DOE Symposium on Improved Oil Recovery, Tulsa, Oklahoma, USA, 22-26 April. SPE-99848-MS. doi:10.2118/99848-MS.
- Handy, L. L., Amaefule, J. O., Ziegler, V. M., et al. 1982. Thermal Stability of Surfactants for Reservoir Application (includes associated papers 11323 and 11597) *SPE J.* **22** (05): 722-909. SPE-7867-PA. doi:10.2118/7867-PA.
- Hayes, M., Bourrel, M., El-Emary, M., et al. 1979. Interfacial Tension and Behavior of Nonionic Surfactants. *SPE J.* **19**: 349–356. doi:10.2118/7581-PA.
- Hezave, A.Z., Dorostkar, S., Ayatollahi, S., et al. 2013. Investigating the effect of ionic liquid (1-dodecyl-3-methylimidazolium chloride ([C12mim] [Cl])) on the water/oil interfacial tension as a novel surfactant. *Colloids Surfaces A Physicochem. Eng. Asp.* **421**: 63–71. doi:10.1016/j.colsurfa.2012.12.008.
- Jeff, R. and Wasan, D. 1993. Surfactant-Enhanced Alkaline Flooding: Buffering at Intermediate Alkaline pH. *SPE Reserv. Eng.* **8**: 275–280. doi:10.2118/21027-PA.
- Karimi, A., Fakhroueian, Z., Bahramian, A. et al. 2012. Wettability alteration in carbonates using zirconium oxide nanofluids: EOR implications. *Energy & Fuels* **26** (2): 1028–1036. doi:10.1021/ef201475u.
- Khezrnejad, A., James, L.A., and Johansen, T.E., 2015. Nanofluid Enhanced Oil Recovery – Mobility Ratio, Surface Chemistry, or Both? International Symposium of the Society of Core Analysts, St. John's Newfoundland and Labrador, Canada, 16-21 August. SCA2015-028.
- Maini, B. B. and Ma, V. 1985. Thermal Stability of Surfactants for Steamflood Applications. SPE Oilfield and Geothermal Chemistry Symposium, Phoenix, Arizona, 9-11 March. doi:10.2118/13572-MS.
- Mohammed, M. and Babadagli, T. 2014. Alteration of Matrix Wettability During Alternate Injection of Hot-water/Solvent into Heavy-oil Containing Fractured Reservoirs. SPE Heavy Oil Conference, Calgary, Alberta, Canada, 10-12 June. doi:10.2118/170034-MS.
- Mohammed, M. and Babadagli, T. 2015. Wettability Alteration: A Comprehensive Review of Materials/Methods and Testing the Selected Ones on Heavy-Oil Containing Oil-Wet Systems. *Adv. Colloid Interface Sci.* **220**: 54–77. doi:10.1016/j.cis.2015.02.006.
- Motealleh, S., de Zwart, B.R., and Bruining, H. 2005. Wettability alteration effects in steam recovery from matrix blocks in fractured reservoirs. 13th European Symposium on Improved Oil Recovery, Budapest, Hungary, 25–27 April.
- Roustaei, A., Moghadasi, J., Bagherzadeh, H., et al. 2012. An experimental investigation of polysilicon nanoparticles' recovery efficiencies through changes in interfacial tension and wettability alteration. SPE Int. Oilf. Nanotechnol. Conf., Noordwijk, Netherlands, 12-14 June. doi:10.2118/156976-MS.

- Sanz, C. A. and Pope, G. A. 1995. Alcohol-Free Chemical Flooding: From Surfactant Screening to Coreflood Design. SPE International Symposium on Oilfield Chemistry, San Antonio, Texas, 14-17 February. doi:10.2118/28956-MS
- Sharma, J. and Gates, I.D. 2013. Interfacial Stability of In-Situ Bitumen Thermal Solvent Recovery Processes. *SPE J.* **16**: 55–64. doi:10.2118/130050-PA.
- Standnes, D.C. and Austad, T. 2003. Wettability alteration in carbonates: Interaction between cationic surfactant and carboxylates as a key factor in wettability alteration from oil-wet to water-wet conditions. *Colloids Surfaces A Physicochem. Eng. Asp.* **216**: 243–259. doi:10.1016/S0927-7757(02)00580-0.
- Wade, W.H., Morgan, J.C., Jacobson, J.K., et al. 1977. Low Interfacial Tensions Involving Mixtures of Surfactants. *SPE J.* **17**: 7–8. doi:10.2118/6002-PA.
- Wagner, O.R. and Leach, R.O. 1966. Effect of Interfacial Tension on Displacement Efficiency. *SPE J.* **6**. doi:10.2118/1564-PA.
- Wang, Y., Xu, H., Yu, W., et al. 2011. Surfactant induced reservoir wettability alteration: Recent theoretical and experimental advances in enhanced oil recovery. *Pet. Sci.* **8**: 463–476. doi:10.1007/s12182-011-0164-7.
- Wasan, D.T. and Nikolov, A.D. 2003. Spreading of nanofluids on solids. *Nature* **423**: 156–159. doi:10.1038/nature01591.
- Wei, Y. and Babadagli, T. 2016. Selection of Proper Chemicals to Improve the Performance of Steam Based Thermal Applications in Sands and Carbonates. SPE Latin America and Caribbean Heavy and Extra Heavy Oil Conference, Lima, Peru, 19-20 October. doi:10.2118/181209-MS.